

## Impact of heterogeneous ice nuclei on homogeneous freezing events in cirrus clouds

P. Spichtinger<sup>1</sup> and D. J. Cziczo<sup>1,2</sup>

Received 1 April 2009; revised 17 March 2010; accepted 2 April 2010; published 29 July 2010.

[1] The influence of initial heterogeneous nucleation on subsequent homogeneous nucleation events in cirrus clouds is investigated using a box model which includes the explicit impact of aerosols on the nucleation of ice crystals and a new sedimentation scheme. Different effects are discussed, namely the impact of external versus internal mixtures of heterogeneous ice nuclei and the influence of size-dependent freezing thresholds. Several idealized experiments are carried out, which show that the treatment of external mixtures of ice nuclei can strongly change subsequent homogeneous nucleation events (i.e., the ice crystal number densities) over a large variety of environmental conditions relevant for the upper troposphere. In most cases a strong reduction in ice crystal number concentrations formed in subsequent homogeneous freezing events is observed. The use of size-dependent freezing thresholds can change cloud properties when compared to more simple parameterizations and is most important at largest ice nuclei concentrations.

**Citation:** Spichtinger, P., and D. J. Cziczo (2010), Impact of heterogeneous ice nuclei on homogeneous freezing events in cirrus clouds, *J. Geophys. Res.*, 115, D14208, doi:10.1029/2009JD012168.

### 1. Introduction

[2] Cirrus clouds are important modulators of Earth's radiation budget. The overall effect of cirrus clouds on the Atmosphere-Earth system is still unknown, but a contribution to a net warming is possible [Chen *et al.*, 2000]. The radiative impact of cirrus clouds is determined by microphysical (e.g., ice crystal number density and ice water content) as well as environmental properties (e.g., temperature and relative humidity). Both net warming induced by thin cirrus clouds or net cooling by thick cirrus clouds is possible. A recent study [Fusina *et al.*, 2007] shows that under certain conditions the transition between net warming and cooling seems to depend crucially on ice crystal number density. Thus, there is a need to know the ice crystal number densities inside cirrus clouds so that a better estimation of a mean radiative impact and possible feedbacks in a warmer climate can be derived.

[3] In the low temperature regime ( $T < 235$  K) homogeneous freezing of aqueous solution droplets [see, e.g., Koop *et al.*, 2000], is highly dependent on the vertical velocity and temperature [see, e.g., Kärcher and Lohmann, 2002; Spichtinger and Gierens, 2009a; Barahona and Nenes, 2008]: A nucleation event is triggered by surpassing thresholds of relative humidity with respect to ice (for different sizes of solution droplets) and is shut down by effective

temperature-dependent depositional growth of ice crystals, which depletes water vapor and thus reduces ice supersaturation. The shutdown of nucleation depends on the competition of source and sink of ice supersaturation (adiabatic cooling versus depositional growth, see section 4.1 for details).

[4] Local dynamics are not the only factor that can change the ice crystal number densities. Previous studies have considered the impact of heterogeneous nucleation, or, more precisely, the competition of different nucleation processes, within the same environment. Box model studies indicate possible suppression of homogeneous nucleation [DeMott *et al.*, 1997; Gierens, 2003; Ren and Mackenzie, 2005] by heterogeneous nucleation. In these studies sedimentation of ice crystals was not considered. Recent cloud resolving simulations [Kärcher, 2005; Spichtinger and Gierens, 2009a, 2009b, 2009c] show that sedimentation is one of the key processes for structuring cirrus clouds and thus should be considered. In general, these studies suggest heterogeneous nucleation preceding homogeneous nucleation events within the same environment can strongly modify those events. That is to say, ice crystal number densities are often significantly reduced when compared to pure homogeneous nucleation events. This effect has been termed the "negative Twomey effect" [Kärcher and Lohmann, 2003; Kärcher *et al.*, 2007]. These results have also been supported by large-scale simulations of the competition between heterogeneous and homogeneous nucleation within the same environment [Kärcher and Lohmann, 2003; Lohmann *et al.*, 2004; Hendricks *et al.*, 2005; Kärcher *et al.*, 2006; Lohmann *et al.*, 2008]. Other box model studies suggest no support of the negative Twomey effect [Kay *et al.*, 2007].

<sup>1</sup>Institute for Atmospheric and Climate Science, ETH Zurich, Zurich, Switzerland.

<sup>2</sup>Now at Atmospheric Sciences and Global Change Division, Pacific Northwest National Laboratory, Richland, Washington, USA.

[5] Almost all of these studies used heterogeneous ice nuclei (IN) represented by idealized internal mixtures with a single distinct activation threshold. From measurements in the troposphere [e.g., *DeMott et al.*, 2003a; *Cziczo et al.*, 2004a] we know that IN often occur in external mixtures with very different components. As a consequence, the freezing properties of these mixtures are very different; each component could have its own characteristic freezing threshold depending on chemical and/or microphysical properties. It is known from laboratory studies that the size of IN also plays a crucial role; larger particles activate as ice crystals at lower relative humidities than smaller particles [*Pruppacher and Klett*, 1997; *Archuleta et al.*, 2005; *Kanji and Abbatt*, 2006; *Marcilli et al.*, 2007]. A priori, it is not clear how these different heterogeneous IN properties will affect homogeneous nucleation occurring later within the same environment.

[6] Recently, laboratory measurements were used to parameterize the freezing properties of different aerosols (e.g. mineral dust, soot) in terms of freezing onset, nucleation rates and contact angle [*Eastwood et al.*, 2008; *Chen et al.*, 2008; *Zimmermann et al.*, 2008]. These measurements are also used to parameterize heterogeneous nucleation for model studies [*Phillips et al.*, 2008; *Eidhammer et al.*, 2009]. However, these studies mostly do not treat external mixtures of different types of IN and the impact of size on the freezing conditions. Additionally, the impact of heterogeneous nucleation events on following homogeneous freezing events has not been taken into account.

[7] In cloud-resolving simulations using only a single heterogeneous IN type it has been shown that the competition of different freezing mechanisms occasionally leads to high ice supersaturation inside cirrus clouds [*Spichtinger and Gierens*, 2009c] by weakening dominant homogeneous nucleation. The behavior of external mixtures of IN may help contribute to a better understanding of the puzzling issue of high and persistent ice supersaturation found inside cirrus clouds [*Peter et al.*, 2006].

[8] Using these issues as motivation, here we study different IN types and size dependent freezing properties in idealized model simulations. Our goal is to give a qualitative and, in some cases roughly quantitative, impression of the effects on homogeneous nucleation events. Size and composition effects on ice nucleation have been understood for some time [e.g., *Pruppacher and Klett*, 1997]. Our intention is not to exactly mimic any specific IN types but to instead understand the general effect of considering several different types and sizes realistically constrained by laboratory and field data. In our simulations we use a box model for classical adiabatic cooling events induced by a constant vertical updraft. This simple framework is used to evaluate the more complex interaction of nucleation mechanisms and IN in detail. Using a Lagrangian viewpoint analysis of the competition of different processes (e.g., cooling, growth, sedimentation) is possible using time derivatives of relative humidity. To overcome problems associated with a lack of sedimentation in classical box model studies on this topic [e.g., *Gierens*, 2003], we implemented a new concept for including the effect of sedimenting ice crystals via a “sedimentation flux”. Further, we have developed a new parameterization for heterogeneous nucleation including size effects.

This scheme is based on a recently developed and validated ice microphysics scheme [*Spichtinger and Gierens*, 2009a] which allows the treatment of arbitrarily many classes of ice and/or ice formation mechanisms which can include the properties of background aerosols.

## 2. Model Description

[9] For this study we use a box model with recently developed ice microphysics (for a detailed description, refer to *Spichtinger and Gierens* [2009a]) extended for heterogeneous nucleation and sedimentation. The basic ice microphysics are described briefly in section 2.1, the new approach for including sedimentation in the box model is described in section 2.2 and the parameterization of size-dependent heterogeneous ice nucleation is presented in section 2.3.

### 2.1. Basic Microphysics

[10] A double-moment bulk microphysics scheme is utilized, i.e., prognostic equations are solved for ice crystal number and mass concentrations, respectively. Ice crystal masses (or equivalently sizes) are assumed to obey lognormal distributions with temporary varying mean mass but a prescribed constant width. Crystal shapes are droxtals (aspect ratio 1) up to a diameter of 7.42  $\mu\text{m}$  and columns with size-dependent aspect ratio for larger sizes. An arbitrary number of ice classes can be treated by this scheme. Each ice class is explicitly tied to an aerosol type that nucleates it, hence ice classes are distinguished by their formation mechanism (e.g., heterogeneously versus homogeneously formed ice). The aerosol types are also described by their number and mass concentration.

[11] In the original model [*Spichtinger and Gierens*, 2009a] the following microphysical processes are parameterized in order to simulate cold cirrus clouds: Nucleation (homogeneous and heterogeneous, see section 2.3), diffusional growth/evaporation and sedimentation. Only recently, the microphysical scheme was validated in a very rigorous way in comparison to in situ measurements of orographic wave clouds [*Gayet et al.*, 2004] in cloud-resolving simulations. The agreement of ice crystal number concentrations, relative humidity over ice and ice water content was excellent [*Joos et al.*, 2009].

[12] The approach for sedimentation within the framework of the box model is described in section 2.2. Ice crystal aggregation is not included in this scheme, because it is of minor importance for the treatment of cold cirrus clouds ( $T < 235$  K) and for low vertical and terminal velocities [*Kajikawa and Heymsfield*, 1989], as is the case in these studies.

[13] For the representation of homogeneous freezing of aqueous solution droplets we prescribe lognormally-distributed sulfuric acid drops as a background aerosol. The water content of the solution droplets is computed using Köhler theory. Freezing rates are calculated using the water activity based and temperature dependent parameterization of *Koop et al.* [2000]. For parameterizing of the diffusional growth of ice crystals, we use a modified approximation of single ice crystal mass rates from *Koenig* [1971] with corrections for small crystals (i.e., droxtals) and ventilation.

## 2.2. Sedimentation Within a Box Model Framework

[14] Classical box models are designed as zero-dimensional models. An air parcel is moved vertically (up/down) but the parcel itself is treated as a closed system. Thus, cloud particles are kept in the box and no sedimentation of hydrometeors occurs [see, e.g., *Gierens, 2003; Hoyle et al., 2005*]. However, studies with cloud-resolving models [e.g., *Spichtinger and Gierens, 2009b, 2009c*] or models including at least the vertical dimension [e.g., *Lin et al., 2005; Kärcher, 2005; Comstock et al., 2008*] show that sedimentation is a key process in shaping the formation and structure of cirrus clouds in systems driven by large-scale motions. Hence, sedimentation should also be included in box models as done in some studies [e.g., *Haag and Kärcher, 2004; Kay et al., 2006*]. However, in most classical box model studies on the competition of heterogeneous and homogeneous nucleation without including sedimentation [e.g., *Gierens, 2003; Ren and Mackenzie, 2005; Barahona and Nenes, 2009*] the impact of heterogeneous nucleation could be overestimated because the ice crystals formed from heterogeneous IN would stay in the box and can deplete water vapor and thus decrease ice supersaturation efficiently. They should, however, fall out quickly, because they are not very numerous and can therefore grow in the supersaturated environment to very large crystals, which have large terminal velocities. Thus a small amount of heterogeneously formed ice crystals could suppress homogeneous nucleation, if they stay within the box, leading to an overestimation of suppression of homogeneous freezing. In the following we describe our approach of implementing sedimentation into a box model; the relation to sedimentation schemes used in former box models studies is discussed in Appendix B.

[15] Instead of a zero-dimensional parcel we prescribe a vertical thickness ( $\Delta z$ ) of the box. For calculating the sedimentation of cloud ice of a specific class we use a one-dimensional implicit advection scheme as used in large-scale models [e.g., *Rotstajn, 1997*]. A scalar quantity  $\psi$  (i.e. cloud ice mixing ratio,  $q_c$  or ice crystal number density,  $N_c$ , respectively) is transported for subsequent time steps  $t_n, t_{n-1}$  ( $\Delta t = t_n - t_{n-1}$ ) in the following way:

$$\psi(t_n) = \psi(t_{n-1}) \cdot e^{-\alpha_\psi} + \frac{R_\psi}{\rho \cdot v_\psi} \cdot (1 - e^{-\alpha_\psi}) \quad (1)$$

Here,  $v_\psi$  is the terminal velocity for the quantity  $\psi$ ,  $\alpha_\psi = \frac{v_\psi \cdot \Delta t}{\Delta z}$  denotes the Courant number,  $\rho$  is the density of dry air and  $R_\psi$  represents the flux from above inside the box through the upper boundary. In our parameterization we use different size-dependent terminal velocities for the quantities cloud ice mixing ratio and ice crystal number density, respectively, i.e. mass-weighted and number-weighted terminal velocities  $v_{q_c}, v_{N_c}$  ( $\psi = q_c, \psi = N_c$ ), respectively,

$$v_{q_c} := \frac{1}{q_c} \int_0^\infty f(m) m v(m) dm, \quad v_{N_c} := \frac{1}{N_c} \int_0^\infty f(m) v(m) dm \quad (2)$$

using the mass distribution of ice crystals  $f(m)$  and the terminal velocity for single ice crystal  $v(m)$ , as already described by *Spichtinger and Gierens* [2009a, section 3.4].

[16] This implicit advection approach can only work in a non-trivial manner with information about the flux  $R_\psi$  from

the layers above. In the case of a box model, because of its zero dimensionality, *a priori* there is no determination of the flux through the top of the layer inside the box, i.e. this flux must be estimated. In a first approximation we assume that the flux through the top is equal to a fraction of the flux through the bottom

$$R_\psi = \psi \rho v_\psi \cdot f_{sed} \quad (3)$$

whereas  $f_{sed}$  specifies the ratio between the fluxes, i.e.  $f_{sed} = (\text{flux through top})/(\text{flux through bottom})$ . The sedimentation scheme as described in equation (1) can be reformulated as follows:

$$\psi(t_n) = \psi(t_{n-1}) \cdot (f_{sed} + (1 - f_{sed}) \exp(-\alpha_\psi)) \quad (4)$$

and can be interpreted in the following way for different values of  $f_{sed}$ .

[17] 1. For  $f_{sed} = 0$ , there is no flux from the top inside the layer, i.e. all ice crystals (mass and number concentration) formed inside the box by nucleation will fall through the bottom of the layer (representing a sink) and there is no source for ice crystal mass or number concentration from layers above; this leads to a net loss of ice crystals.

[18] 2. For  $0 < f_{sed} < 1$ , there is a flux from the top layers inside the box, but the flux through the bottom of the layer (i.e. the sink) is larger than the flux through the top of the layer (i.e. the source), leading to a net loss of ice crystals; however, the loss is decreasing with increasing  $f_{sed}$ .

[19] 3. For  $f_{sed} = 1$ , the flux from above inside the box is in balance with the flux through the bottom, i.e. the box is in equilibrium. This scenario is equivalent to the classical box model approach where no sedimentation is included.

[20] 4. For  $f_{sed} > 1$ , the flux from above is larger than the loss of ice crystals by sedimentation through the bottom of the box, this lead to a net gain of ice in the box. For long simulations this will lead to unphysical behavior, filling the whole box with ice.

[21] For realistic cloud simulations the parameter  $f_{sed}$  should be in the range  $0 \leq f_{sed} \leq 1$  inside the cloud, while the extreme case  $f_{sed} = 0$  only makes physical sense for simulations of the cloud top layer. From cloud resolving model studies [e.g., *Spichtinger and Gierens, 2009a, 2009b, 2009c*] we can estimate the ratio of the fluxes through the top and the bottom of a single layer. At the cloud top, especially in regions with continuous and strong nucleation the parameter  $f_{sed}$  is in the range  $0 < f_{sed} < 0.6$ . For regions inside a cirrus cloud dominated by ice crystal falling from top layers, growing inside the box and falling through the bottom, the parameter  $f_{sed}$  is near unity. At the bottom of the cloud, especially if the layers below the cloud are strongly subsaturated, values  $f_{sed} > 1$  could be possible. In this case ice crystals fall into subsaturated air and evaporate (partly). Thus, they fall slower and their mass is reduced, leading to a smaller flux through the bottom than through the top, i.e.  $f_{sed} = (\text{flux through top})/(\text{flux through bottom}) > 1$ .

[22] Alternatively, this parameter  $f_{sed}$  could be used as an *a priori* constraint to the box model as a determinate for which part of the cirrus cloud the simulations are representative. By thus specifying the value of  $f_{sed}$  the box model calculations are representative of the described regions. The

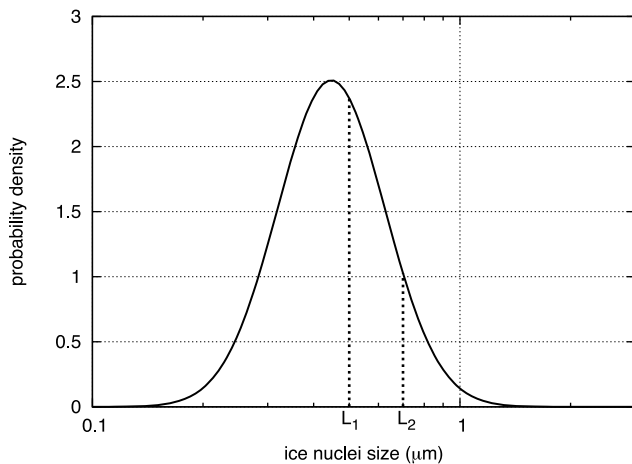


**Figure 1.** Normalized size distribution for ice nuclei and determination of the amount of newly formed ice crystals from the size distribution for the heterogeneous ice nuclei. The amount is calculated by using the integral over the distribution with lower and upper boundary  $L_1$ ,  $L_2$ , respectively. The modal size and the width of the size distribution of log-normal type ( $L_m = 0.5 \mu\text{m}$ ,  $\sigma = 1.4$ ) were derived from the “Storm Peak” measurements [DeMott *et al.*, 2003a].

caveat here is that this also restricts the results to one specific region, specified by the sedimentation flux ratio  $f_{sed}$  of the cloud whereas box model calculations are normally not restricted in this manner [e.g., Gierens, 2003; Haag and Kärcher, 2004; Kay *et al.*, 2006, 2007]. This is especially true for the extreme cases  $f_{sed} = 0$  and  $f_{sed} = 1$ , which have often been used without detail of the sedimentation process.

[23] In our simulations we specify the value of  $f_{sed}$  for two cases. First, we consider the case of cloud top layers, i.e.,  $f_{sed} = 0.5$ . Second, we specify  $f_{sed} = 0.9$ , i.e. these simulations are representative of the situation inside a cirrus cloud, i.e. in the middle of a cloud. This region, dominated by growth and sedimentation, is similar to the reference cases from Spichtinger and Gierens [2009b], but with a net loss of ice crystals. Furthermore, the approach of using two terminal velocities (mass and number weighted, depending on mean ice crystal mass) guarantees that larger ice crystals fall out earlier than smaller ones [see Spichtinger *et al.*, 2006; Wacker and Seifert, 2001], as would be expected in nature. This is due to the fact that the mass weighted terminal velocity is always larger than the number weighted terminal velocity [Spichtinger *et al.*, 2006; Spichtinger and Gierens, 2009a].

[24] In some earlier box model studies sedimentation was included, i.e. the approach of  $f_{sed} = 0$  was used [e.g., Haag and Kärcher, 2004; Kay *et al.*, 2006, 2007]. In these studies the vertical depth of the box was changed in order to obtain different regimes of sedimentation. Both approaches, ours and the former one are almost equivalent as is discussed in Appendix B; however, some principal advantages of our approach are also mentioned there.

### 2.3. Heterogeneous Nucleation Parameterizations

[25] We use two different parameterizations of heterogeneous nucleation. The first, more simple, parameterization

was previously used by Spichtinger and Gierens [2009c]: A threshold of relative humidity for the activation of available IN is prescribed. If the environmental relative humidity surpasses this threshold value  $RHi_{het}$ , all background aerosol particles are activated as IN and form ice crystals of an initial size. Ice crystals then grow by diffusional growth. Due to its simplicity this type of parameterization is commonly used in large-scale models (e.g., here  $RHi_{het} = 130\%$  [Lohmann *et al.*, 2004]).

[26] Although laboratory and field measurements sometimes indicate a threshold behavior of the onset of heterogeneous nucleation, they also indicate that the size of an aerosol is an important factor in their ability to act as IN [Archuleta *et al.*, 2005; Marcolli *et al.*, 2007]. Specifically, it appears that larger aerosols activate at lower supersaturations than smaller ones. Therefore, the following parameterization has been developed.

[27] A size (or even mass) distribution  $f(L)$  for the background aerosol assigned to a specific class of ice is prescribed. A size-dependent activation threshold  $RHi_{het}(L)$  is then chosen as a monotone function. Thus, for each aerosol of a specific size  $L$  there is exactly one nucleation threshold  $RHi_{het}(L)$ . Generally, the following equation must be fulfilled, mimicking the measurements:

$$RHi_{het}(L_1) > RHi_{het}(L_2) \text{ for } L_1 < L_2. \quad (5)$$

The amount of newly nucleated ice crystals is calculated by:

$$\Delta N_i = N_a \cdot \int_{L_1}^{L_2} f(L) dL \quad (6)$$

at every time step, as indicated in Figure 1. Note that the size distribution is cut off at the tail of large aerosol particles during a nucleation event. For the calculation the monotony of the function  $RHi(L)$  is used for determining the unique inverse function  $L(RHi)$ , which is then used for determining the nucleated amount of ice crystals from the actual relative humidity. Ice crystals will only be formed if  $L(RHi(t_n)) < L(RHi(t_{n-1}))$  for succeeding time steps  $t_n > t_{n-1}$ . In our parameterizations we use functions of the form  $RHi(L) = (a/L)^b + RHi_0$  which fulfill the constraints mentioned above. The  $RHi(L)$  function was modeled after the measurements by Archuleta *et al.* [2005]. Here, parameter  $b$  determines the curvature of the curve, parameter  $a$  is used for scaling purposes.

[28] For comparing these parameterizations with the simple constant threshold a mean threshold  $RHi_{mean}$  can be derived by:

$$RHi_{mean} = \int_0^{\infty} f(L) RHi(L) dL \quad (7)$$

[29] For the investigation of the impact of internal versus external mixtures of IN and/or the additional impact of the size of IN we specify five different cases for our simulations. In the reference case (“hom”), we consider only homogeneous freezing of supercooled aqueous solution droplets [Koop *et al.*, 2000]. In order to determine size-

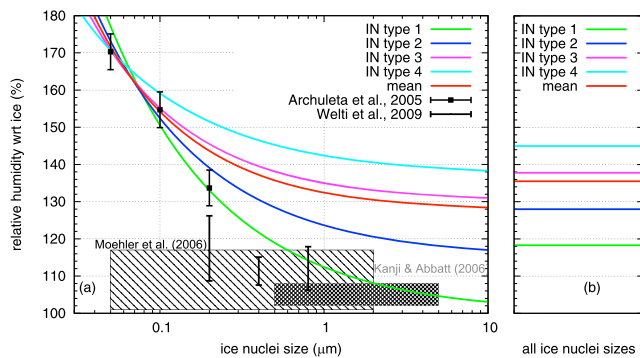


**Figure 2.** Freezing thresholds for (a) size-dependent heterogeneous nucleation and (b) step heterogeneous parameterization. For internally mixed IN the type “mean” indicates the threshold behavior. The two parameterizations including this class are termed “step(1)” and “size(1)”, respectively. For externally mixed IN the nucleation thresholds for the four used classes of IN are indicated by the curves “IN type 1, 2, 3, 4”, respectively. The parameterizations including these types of IN are termed “step(4)” and “size(4)”, respectively. The constant values of each type of IN (mean, IN type 1–4) in Figure 2b are calculated using the corresponding curves (Figure 2a) in equation (7). The black and gray rectangles indicate the range of freezing thresholds as found in laboratory measurements by Möhler *et al.* [2006] (black) and Kanji and Abbatt [2006] (gray), respectively.

dependent parameterization for the nucleation threshold we use a general size distribution of lognormal type:

$$f(L) = \frac{N}{\sqrt{2\pi} \log \sigma_L} \exp\left(-\frac{1}{2} \left(\frac{\log(L/L_m)}{\log \sigma_L}\right)^2\right) \frac{1}{L}. \quad (8)$$

The parameters for the distribution were obtained from observations at the Desert Research Institute Storm Peak Laboratory located in north-central Colorado in the US Rocky Mountains [DeMott *et al.*, 2003a; Cziczo *et al.*, 2003, 2006; Richardson *et al.*, 2007] and are set to  $L_m = 0.5 \mu\text{m}$ ,  $\sigma_L = 1.4$  (see also Figure 1).

[30] We want to investigate the impact of (1) internally versus externally mixed heterogeneous IN and (2) constant versus size-dependent freezing thresholds. For representing these basic cases we use the following parameterizations.

[31] For representing internally mixed IN we use one class of IN. Here, we discriminate between a parameterization with a single threshold (i.e. step-wise parameterization “step(1)”) and a parameterization with a size-dependent threshold (“size(1)”). The step-wise parameterization is represented by the constant value “mean” ( $RHi = 135.5\%$ ) in Figure 2b. This value is comparable to values used in previous large-scale model parameterizations [e.g., Kärcher *et al.*, 2006]. The size-dependent parameterization is represented by the curve “mean” in Figure 2a. Both parameterizations are connected by equation (7), i.e. the constant threshold can be calculated using the size-dependent parameterization. These experiments “step(1)” and “size(1)” are designed for describing a kind of mean IN, i.e. in the

middle between very good IN ( $RHi \sim 100\text{--}110\%$ ) and homogeneous nucleation thresholds.

[32] For representing externally mixed IN we use four different classes of IN. Again we discriminate between a step-wise parameterization (“step(4)”) and a size-dependent parameterization (“size(4)”). In case of constant nucleation thresholds (“step(4)”) the constant values ( $RHi = 118.3/128/137.8/145\%$ ) are represented in Figure 2a (IN type 1–4). The size-dependent nucleation thresholds for the externally mixed IN used for parameterization “size(4)” are shown in Figure 2b (IN type 1–4). Note, that the thresholds for IN types 1–4 can be calculated using the corresponding size-dependent nucleation thresholds in equation (7).

[33] In order to include the impact of size dependent nucleation thresholds (experiments “size(1)” and “size(4)”) we consider the laboratory measurements of ice nucleation by mineral dust [Archuleta *et al.*, 2005; Möhler *et al.*, 2006; Kanji and Abbatt, 2006]. These examples show a dependency of the nucleation threshold of mineral dust on the size of the aerosol particle, a trend apparent for IN in general [Pruppacher and Klett, 1997]. We note that whereas Archuleta *et al.* [2005] investigated monodisperse samples it is known that atmospheric IN are often larger than these [Cziczo *et al.*, 2006]. Therefore, we consider the polydisperse studies of Möhler *et al.* [2006] and Kanji and Abbatt [2006], which extend to larger sizes. Again, our intention here is not to precisely mimic specific aerosol types but to consider the general trends of ice nucleation with respect to size using these laboratory studies for constraints. The different parameterizations for experiments “step(1)”, “size(1)”, “step(4)”, “size(4)”, respectively, are shown in Figure 2 and are also listed in Table 1. Additionally, we listed the reference experiment “hom” which includes homogeneous nucleation only.

[34] Three points are noteworthy. First, these parameterizations make no assumption about the mode of heterogeneous nucleation. Our intention is to observe differences between all heterogeneous nucleation modes and homogeneous freezing. Attempts to distinguish between heterogeneous modes (e.g., deposition, immersion, contact, etc.) are ongoing in laboratory and field studies and beyond the scope of this paper. Second, the size distribution given in Figure 1 reflects the active ice nuclei which should not be confused with the total aerosol. That is to say, only a minor fraction of the background aerosol will act as ice nuclei [DeMott *et al.*, 2003a] and only these are modeled in Figure 1. Third, many research groups have investigated both homogeneous and heterogeneous freezing; recent reviews include that by Cantrell and Heymsfield [2005]. We use data predominantly

**Table 1.** Setup for the Background Aerosol for Different Types of Experiments

Experiment	Number of IN Types	Parameterization Type
hom	0	only hom. nucl. internally mixed IN
step (1)	1	steps, $RHi = 135.5\%$ , “mean” in Figure 2b
size (1)	1	size, “mean” in Figure 2a externally mixed IN
step (4)	4	steps, $RHi = 118.3/128/137.8/145\%$ , IN type 1–4 in Figure 2b
size (4)	4	size, IN type 1–4 in Figure 2a

**Table 2.** Summary of the Variation of All Parameters for the Simulations

Experiment	$T_{init}(K)$	$w(m\ s^{-1})$	$f_{sed}$	Total IN ( $L^{-1}$ )
hom	210	00.05	0.5	14 (normal)
step(1)	220	00.10	0.9	140 (polluted)
size(1)	230	00.15		
step(4)	240	00.20		
size(4)				

from Archuleta *et al.* [2005], Möhler *et al.* [2006], Kanji and Abbatt [2006] and DeMott *et al.* [2003a]. Our intention is to use recent data sets to provide an idealized size- and composition-dependent theory framework ice nucleation. For example, the nucleation thresholds are meant to mimic compositional effects observed by DeMott *et al.* [2003a] and the size distribution of IN is an idealized distribution from the “Storm Peak” observations of Cziczo *et al.* [2006]. A complete review or synthesize of all laboratory and field data available is beyond the scope of this work.

### 3. Setup

[35] In all experiments an updraft of constant vertical velocity  $w$  inducing adiabatic cooling of  $dT/dt = -g/c_p \cdot w$  is prescribed. Pressure is changed consistently. For testing the sensitivity according to the vertical velocity the following values were used:  $w = 0.05, 0.10, 0.15, 0.2\ m\ s^{-1}$ , respectively. Although only slow large-scale motion (i.e.  $w \leq 0.1\ m\ s^{-1}$ ) are mentioned here, the velocity range has also been extended to higher values, representing moderate mesoscale vertical velocities [see, e.g., Spichtinger *et al.*, 2005b]. The total simulation time is chosen such that during the simulation the air parcel experiences a total altitude difference of  $\Delta z = 1800\ m$ . This translates to simulation times of  $\Delta t = 600/300/200/150\ min$  for vertical velocities of  $w = 0.05/0.1/0.15/0.2\ m\ s^{-1}$ , respectively. The parameters are summarized in Table 2.

[36] The choice of the altitude difference is based on typical durations of large scale ascents ( $w \sim 0.05\ m\ s^{-1}$ ) lasting about 10 hours and producing ascents of about 2 km in the upper troposphere [see, e.g., Spichtinger *et al.*, 2005a]. The scenarios with high vertical upward motions were thus adapted to this choice. The time step was fixed to  $\Delta t = 1\ s$ ; this is a reasonable setup for the ice microphysics in case of vertical velocities  $w \leq 0.2\ m\ s^{-1}$  [see Spichtinger and Gierens, 2009a, section 4.1.3]. For the sedimentation of ice crystals the thickness of the cloud layer has to be specified. Here, a thin layer of  $\Delta z = 50\ m$ , is chosen to be close to cloud-resolving model simulations [Spichtinger and Gierens, 2009b, 2009c].

[37] All simulations start with  $p = 300\ hPa$  and  $RHi = 95\%$ , respectively. For testing the sensitivity to different temperature regimes the initial temperature is set to  $T_{init} = 210/220/230/240\ K$ ; the temperature difference at the end of all simulations is  $\sim 17.5\ K$  compared to the initial state, resulting into a temperature range of  $192.5 \leq T \leq 240\ K$ , which is within the valid range for the microphysics parameterization [Spichtinger and Gierens, 2009a].

[38] For the class of ice representing homogeneously-formed crystals the number density of the background aerosol (i.e., pure sulfuric acid droplets) is set to  $n_{a,hom} =$

$200\ cm^{-3}$ , which is representative for the upper troposphere [see, e.g., Minikin *et al.*, 2003]. For the size distribution of lognormal type for the background aerosol a modal radius of  $r_m = 25\ nm$  and a standard deviation of  $\sigma_r = 1.4$  are prescribed, according to the validation of the microphysics scheme [Spichtinger and Gierens, 2009a].

[39] For the setup of the experiments including heterogeneous nucleation we have to prescribe the total amount of available IN number concentration, which acts as an upper bound for the maximum possible ice crystal number concentration formed by heterogeneous nucleation as given in nature; this model framework is different from some other parameterizations where either the total aerosol is prescribed or even in principal arbitrary many IN can be produced [see, e.g., Meyers *et al.*, 1992].

[40] The IN concentration in the upper troposphere is typically on the order of  $\sim 10\ L^{-1}$  [DeMott *et al.*, 2003a]. However, IN concentrations one order of magnitude higher have been observed [DeMott *et al.*, 2003b]. Therefore, we specify two different types of scenarios: First, we prescribe “clean air” (standard scenario) with a total IN concentration of  $n_{a,total} = 14\ L^{-1}$ . Second, we prescribe a “polluted” scenario, i.e., the total IN concentration is  $n_{a,total} = 140\ L^{-1}$ , similar to a measured polluted case [DeMott *et al.*, 2003b]. For experiments containing only one class of IN (internally mixed) this is also the initial value for the background IN concentration  $n_a = n_{a,total}$ . For experiments containing four types of IN (externally mixed) the total concentration is distributed into the different classes as follows: Class “type 1” contains  $2/14$  of  $n_{a,total}$ , class “type 2” contains  $3/14$  of  $n_{a,total}$ , class “type 3” contains  $4/14$  of  $n_{a,total}$  and class “type 4” contains  $5/14$  of  $n_{a,total}$ , respectively. The distribution of the total IN concentration into the different classes of IN is also shown in Figure 3 for the case of constant thresholds (experiments “step(1)/step(4)”). For size-dependent parameterizations the distribution of the IN is analogous, i.e. the total number concentration is distributed into the four

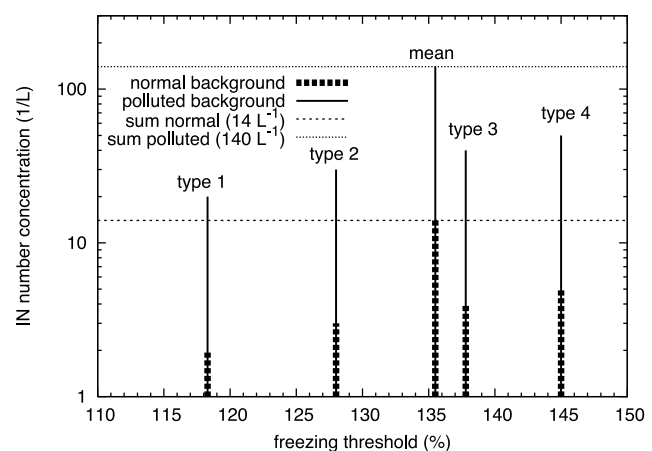


**Figure 3.** Distribution of IN concentration (initialization) for internally and externally mixed IN in the normal and the polluted background. The distribution is exemplary done for step-wise parameterizations (step(1) = mean, step(4) = type 1–4), but for size-dependent parameterizations in experiments “size(1)/size(4)” the distribution of IN to the different modes is the same.

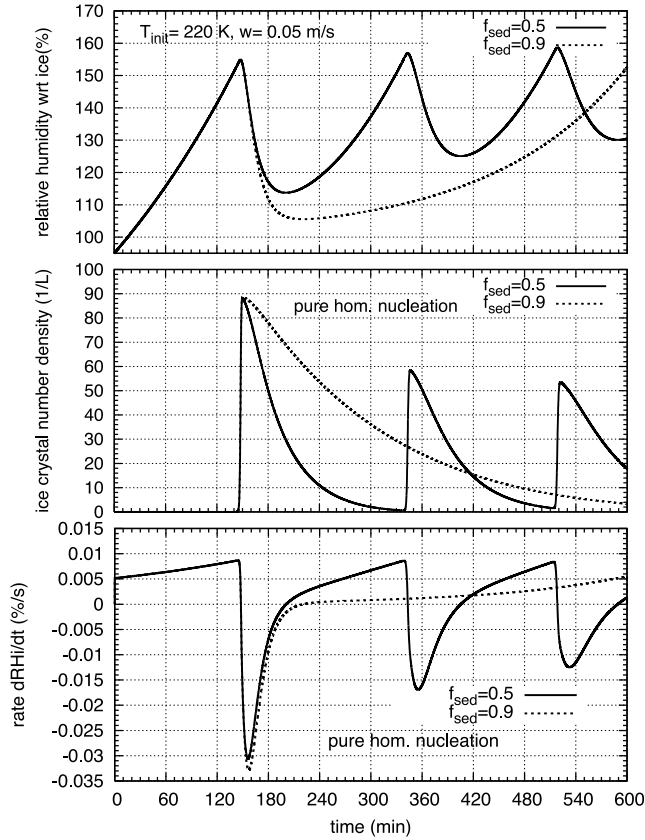


**Figure 4.** (top) Relative humidity over ice (in %), (middle) ice crystal number density (in  $L^{-1}$ ), and (bottom) time derivative of the relative humidity over ice (in %/s) for two different regimes inside the cirrus:  $f_{sed} = 0.5$  representing the top layer of the cloud and  $f_{sed} = 0.9$  representing a layer inside the cirrus dominated by sedimenting ice crystals. Initial conditions for the simulations:  $T_{init} = 220$  K,  $p = 300$  hPa, constant updraft of  $w = 0.05$  m  $s^{-1}$  over the complete simulation duration.

classes of IN as above. Additionally, each class of IN has a size distribution as mentioned above (see also Figure 1); the size distribution could be derived from measurements [Cziczo *et al.*, 2006]. Using this distribution of the IN number concentration we attempt to mimic that IN attributed with a low freezing threshold occur rarely in the upper troposphere. This is likely due to the fact that a low threshold increases the probability that such an aerosol will experience a sufficient relative humidity to freeze and sediment. Thus, IN attributed with a relatively high freezing threshold should occur more frequently.

## 4. Results

### 4.1. Background

[41] First, we describe some basic features of our simulations, i.e. the general impact of sedimentation (section 4.1.1) and the impact of heterogeneous nucleation on a subsequent homogeneous nucleation event (section 4.1.2). These findings are not entirely new and agree very well with former simulations [e.g., Kay *et al.*, 2006]. However, a review of

these basic mechanisms will help us to understand the more complex simulations about the impact of internally versus externally IN mixtures and size-dependent heterogeneous nucleation on homogeneous freezing. Additionally, we focus more on the Lagrangian view including the rate of relative humidity separated into different source/sink terms according to the processes of cooling, growth, and sedimentation.

[42] In clear air the relative humidity is only controlled by the cooling rate, represented by the constant updraft velocity  $w$ . In air masses containing ice crystals, they can deplete water vapor by diffusional growth, acting as a sink for ice supersaturation. If sedimentation of ice crystals is allowed, it will compete with the two other processes (cooling and growth): As soon as ice crystals are large enough to have reasonable terminal velocities (maximum size  $L \geq 15$   $\mu\text{m}$ , resulting into  $v_t(L) \geq 0.01$  m  $s^{-1}$ ), these crystals fall out of the layer, thereby decreasing the sink for ice supersaturation (depositional growth). In terms of rates of relative humidity, this competition can be described formally by splitting the relative humidity rates into components of the processes:

$$\frac{dRH_i}{dt} = \left. \frac{dRH_i}{dt} \right|_c + \left. \frac{dRH_i}{dt} \right|_g + \left. \frac{dRH_i}{dt} \right|_s. \quad (9)$$

The first term represents the source of supersaturation driven by adiabatic cooling (positive sign), the second term denotes the sink of supersaturation due to ice crystal growth (negative sign) and the third term denotes the contribution by sedimenting ice crystals. For the third term, an indirect feedback on relative humidity occurs. Changes in ice crystal mass and number concentrations by sedimentation results into changes of the strength of subsequent growth of ice crystals. Generally, the third contribution could have positive or negative sign: In case of  $f_{sed} < 1$  (all cases in our study) the term is positive, while for net gain of ice crystals ( $f_{sed} > 1$ ) the term is negative. If no sedimentation is allowed ( $f_{sed} = 1$ ), this term vanishes. In Appendix A this formula is motivated by some analytical derivations – valid for our bulk microphysics approach. Equation (9) represents the competition of different sources and sinks of  $RH_i$  (cooling, growth, sedimentation) forming a net rate of  $RH_i$ .

[43] Instead of using time scales, which describe the asymptotic behavior of ice supersaturation (as, e.g., in work by Kay *et al.* [2006]) we decided to investigate the rates of relative humidity over ice, which represents the actual change of relative humidity at a given time. This allows us to analyze the Lagrangian evolution of different variables in more details.

#### 4.1.1. Impact of Sedimentation

[44] The impact of ice crystal sedimentation on the reference simulations (experiment “hom”, i.e. only homogeneous nucleation) is investigated. As an example the case of  $T_{init} = 220$  K and  $w = 0.05$  m  $s^{-1}$  is chosen. In Figure 4 the relative humidity over ice (Figure 4, top), the ice crystal number density formed by homogeneous nucleation (Figure 4, middle) and the rate of relative humidity (Figure 4, bottom) are shown, respectively, for values of  $f_{sed} = 0.5$  (cloud top, solid line) and  $f_{sed} = 0.9$  (middle of cloud, dotted line). These two simulations correspond to the scenarios “fallout dominated” ( $f_{sed} = 0.5$ ) and “limited fallout” ( $f_{sed} = 0.9$ ) in Kay *et al.* [2006], respectively (see also Appendix B).

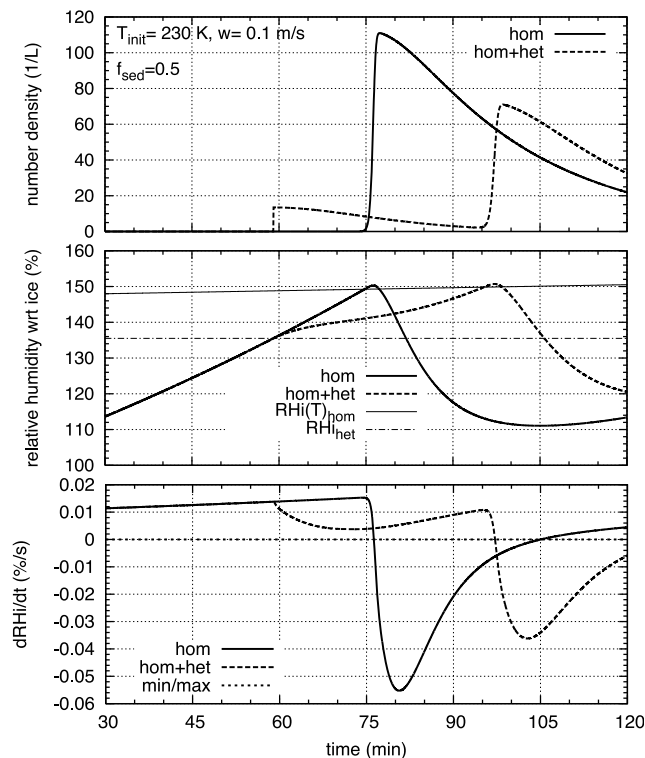


**Figure 5.** For a reference experiment ( $T_{init} = 230$  K, constant updraft of  $w = 0.10$  m s<sup>-1</sup>, IN parameterization “step (1)”), the evolution of (top) ice crystal number density (in L<sup>-1</sup>), (middle) relative humidity over ice (in %) and (bottom) time derivative of the relative humidity over ice (in %/s) is shown. Additionally, the temperature dependent homogeneous freezing threshold  $RHi(T)_{hom}$  is shown (for solution droplets of size  $0.25$   $\mu$ m).

[45] Both simulations are equal until homogeneous nucleation sets it at  $t \sim 145$  min producing a moderate amount of ice crystals ( $n_c \sim 90$  L<sup>-1</sup>). After the nucleation event, growth dominates the simulations, showed clearly in the drastic change of the relative humidity rate, which is strongly negative. For different cloud regimes, determined by the sedimentation fraction  $f_{sed}$  (cloud top:  $f_{sed} = 0.5$ , middle of cloud:  $f_{sed} = 0.9$ ) the ice crystals fall out differently, which results into different behavior for these two regimes. This is clearly represented by the rate  $dRH_i/dt$ .

[46] In the cloud top regime ( $f_{sed} = 0.5$ ) the ice crystals fall out soon after they formed, thus reducing depositional growth, which depletes ice supersaturation. After reaching the minimum at about  $t \sim 156$  min, the rate again increases, indicating the increasing importance of the sedimentation process in removing ice crystals. Due to the steady loss of ice crystals the absolute strength of both processes, growth and sedimentation, respectively, is reduced, until after about  $t \sim 200$  min adiabatic cooling is again the dominant process, slightly modified by the others. Thus, the relative humidity can rise again and after most of formed ice crystals have fallen out, subsequent nucleation events can be triggered. Due to a slightly smaller relative humidity rate at the new nucleation events, the amount of nucleated ice crystals is

smaller than for the first event. This issue will be discussed later in the context of other simulations.

[47] For a large ratio of the sedimentation fluxes ( $f_{sed} = 0.9$ , i.e. middle of cloud) the ice crystals remain in the box longer, thus acting as a supersaturation sink for a longer time. A first indication for this is the slightly deeper and later minimum in the humidity rate (at  $t \sim 157$  min). In this case the ice crystals remain in sufficient number in the box that a kind of quasi steady state is reached in terms of the humidity rate: The combination of the three processes results in an almost constant, slightly positive, humidity rate. This kind of quasi steady state lasts for quite a while and is a very typical feature for cirrus cloud formation under slow synoptic updrafts [see, e.g., Kärcher, 2005; Spichtinger and Gierens, 2009b, 2009c; Comstock et al., 2008]. This basic behavior will have strong impact on the competition between heterogeneous and homogeneous nucleation; it has a large impact on microphysics if a few heterogeneously formed ice crystals stay longer in the box influencing the ice supersaturation or if they fall out soon.

#### 4.1.2. Impact of Heterogeneous Nucleation

[48] From laboratory measurements we know that heterogeneous nucleation takes place at lower freezing thresholds than for homogeneous freezing of solution droplets [e.g., DeMott et al., 2003a]. Indeed, this feature is inherent in all parameterizations for heterogeneous nucleation (see previous sections). For an illustration how heterogeneous nucleation will change the original competition of the different processes during a homogeneous nucleation event as described in section 4.1.1, we investigate a simulation with constant updraft of  $w = 0.1$  m s<sup>-1</sup>, initial temperature  $T_{init} = 230$  K, sedimentation parameter  $f_{sed} = 0.5$ , a step-wise nucleation parameterization (experiment step(1)), used for a better understanding of the process due to its simplicity, and “normal” heterogeneous IN background concentrations ( $n_{total} = 14$  L<sup>-1</sup>). In Figure 5 the time evolution of  $RHi$ , total ice crystal number concentration and  $dRH_i/dt$ , respectively, is shown for experiments “hom” and “step(1)”.

[49] First, the reference case (experiment hom) is described. After the initial phase where adiabatic cooling is dominant, a homogeneous nucleation event is triggered (at  $\sim 75$  min); in Figure 5 the threshold for  $0.25$   $\mu$ m solution droplets is shown ( $RHi_{hom}(T)$ ). Ice crystal growth terminates off the nucleation event by depleting the available water vapor effectively (the rate becomes strongly negative). After a while, sedimentation becomes more important, reducing the sink of supersaturation and leading to an increasing relative humidity rate.

[50] In case of additionally available IN, some changes compared to “hom” can be observed. As in the reference case, during the initial phase of experiment “step(1)” the relative humidity is increasing due to adiabatic cooling, until the threshold for heterogeneous nucleation ( $RHi_{het} = 135.5\%$ ) is reached at about  $t = 59$  min; all available IN are transferred into ice crystals and start to growth. Thus, ice crystal growth competes with cooling in terms of the relative humidity rate (Figure 5, bottom). However, in contrast to the homogeneous nucleation event described above, the amount of formed ice crystal ( $\sim 14$  L<sup>-1</sup>) is too small to turn the rate into a negative one; the relative humidity is still increasing, but with a smaller slope. At around  $t \sim 61$  min, ice crystals

are large enough to have a significant terminal velocity and sedimentation begins to add a positive contribution to the relative humidity rates by slowing the descent and becoming an increasingly important contribution. At around  $t \sim 73$  min the relative humidity rate reaches a minimum representing a local steady state between all three competing processes. At subsequent times, growth of ice crystals is still reduced (according to sedimentation) and from about  $t \sim 80$  min on, adiabatic cooling is again the most important contribution, slightly modified by the remaining ice crystals, leading to an increasing relative humidity. At  $t \sim 95$  min, a homogeneous nucleation event is triggered, however, the amount of formed ice crystals is significantly smaller than in case of the reference simulation (pure homogeneous nucleation). This can be explained as follows. For homogeneous nucleation the amount of formed ice crystals depends crucially on the shape of the relative humidity curve, i.e., on two different properties.

[51] 1. Maximum value of the relative humidity: The freezing rate for homogeneous nucleation depends crucially on the environmental relative humidity (or equivalently on the water activity). The higher the supersaturation the smaller solution droplets can freeze to ice crystals. Thus, the maximum value of an overshooting determines the nucleation event.

[52] 2. Width of the relative humidity peak during a nucleation event: Ice crystals form by freezing solution droplets of a distinct size if the ice supersaturation is above the corresponding threshold for these droplets (depending on temperature and size of the droplets). In other words, the longer the supersaturation remains at high values the more ice crystals can be formed.

[53] The characteristic peak of the overshooting relative humidity during a homogeneous nucleation event is shaped by the processes of cooling and the growth of ice crystals. Effective growth switches off homogeneous nucleation if the relative humidity falls below the activation threshold. Thus, the shape of the relative humidity evolution is the key determinate of the strength of a homogeneous nucleation event.

[54] In our basic example, the shape of the relative humidity evolution is changed by the earlier heterogeneous nucleation event when compared to the reference case without heterogeneous nucleation. The width of the nucleation peak in both cases (at  $t \sim 75$  min for pure homogeneous nucleation and  $t \sim 95$  min including heterogeneous IN, respectively) is comparable but the slope of the curve is different, as showed in the time evolution of  $dRH_i/dt$  (see Figure 5, bottom). This leads to a reduced amount of homogeneously formed ice crystals after heterogeneous nucleation when compared to the reference case. Heterogeneous nucleation can thus modify homogeneous nucleation by changing the sink and source terms growths and sedimentation, respectively, therefore leading to a different time evolution of  $RH_i$  and  $dRH_i/dt$ . It should be noted that the change of the slope of  $dRH_i/dt$  is only one possibility means to influence homogeneous nucleation. It is later shown in cases of a strongly polluted environment that the value of  $dRH_i/dt$  alone does not provide a complete answer and that the evolution of  $RH_i$  and  $dRH_i/dt$  sometimes also must be considered.

## 4.2. Two Case Studies

[55] After this qualitative investigation of the possible impact of heterogeneous IN on homogeneous nucleation the impact of different parameterizations for heterogeneous nucleation is considered. Initially, two series of simulations (experiments “hom, step(1), size(1), step(4), size(4)”) are investigated for a qualitative overview on the impact of different IN parameterizations, using  $T_{init} = 230$  K,  $p = 300$  hPa,  $w = 0.1$  m s<sup>-1</sup> and  $f_{sed} = 0.5/0.9$ , respectively.

[56] In Figure 6 the evolution of the relative humidity (Figure 6, top) and the ice crystal number density (lower row) for different experiments (“hom, step(1), size(1), step(4), size(4)”) and sedimentation fluxes (left column:  $f_{sed} = 0.5$ , right column:  $f_{sed} = 0.9$ ) is shown. First, the impact of size-dependent versus step-wise parameterizations for internally mixed IN (experiment “size(1) versus step(1)”) in the cloud top scenario ( $f_{sed} = 0.5$ ) is investigated in comparison to the reference experiment (“hom”). First, in all cases the relative humidity increases due to constant adiabatic cooling. At around  $t \sim 54$  min, in experiment “size(1)” the first ice crystals are formed, which affect the relative humidity rate by ice crystal growth, as shown in Figure 7 (top). In experiment “step(1)” the onset of nucleation is later, at  $t \sim 59$  min. However, the changes in the rate  $dRH_i/dt$  are similar in both experiments, although for the step-wise parameterizations the changes are more abrupt than for the size-dependent parameterization, as expected. In principle, both experiments behave similarly to the case described in section 4.1.2, thus the rates increase again after sedimentation becomes more important until a homogeneous nucleation event is triggered at  $t \sim 94$  min. The strength of the nucleation event (i.e. the total amount of formed ice crystals) is reduced due to the change in the relative humidity rate (see Figure 7). In the subsequent simulation time, the relative humidity of experiments “step(1)” and “size(1)”, respectively, meet the reference experiment (“hom”) at around  $t \sim 160$  min and after that similar ice crystal number concentrations are produced in following nucleation events. However, the direct match of the curves is accidental. More often a kind of “phase change” or time shift of the  $RH_i$  evolution is observed. The curves (“hom” versus “step(1)/size(1)”) have the same shape (and almost the same amount of ice crystals is produced) but they are shifted in time. This effect is a general feature observed in many simulations and is discussed in section 5. The differences between the experiments “step(1)” and “size(1)” in terms of ice crystal number concentration and relative humidity are marginal.

[57] Next, the experiments including four different types of heterogeneous IN are considered (“step(4), size(4)”), representing externally mixed IN. In both cases, heterogeneous nucleation occurs quite early due to relatively low freezing thresholds. The size-dependent parameterization starts to form ice crystals first (around  $t \sim 27$  min), whereas the step-wise parameterization is switched on discretely; this behavior can be seen in the rate  $dRH_i/dt$  for experiment “step(4)”, with nucleation steps at  $t \sim 36/50/65/78$  min, respectively. Although the ice crystal number density increases slowly and is decreased by sedimentation, the relative humidity is changed significantly when compared to the experiment “hom”. The increase in the supersaturation is markedly reduced, as also shown in Figure 7 (top). The

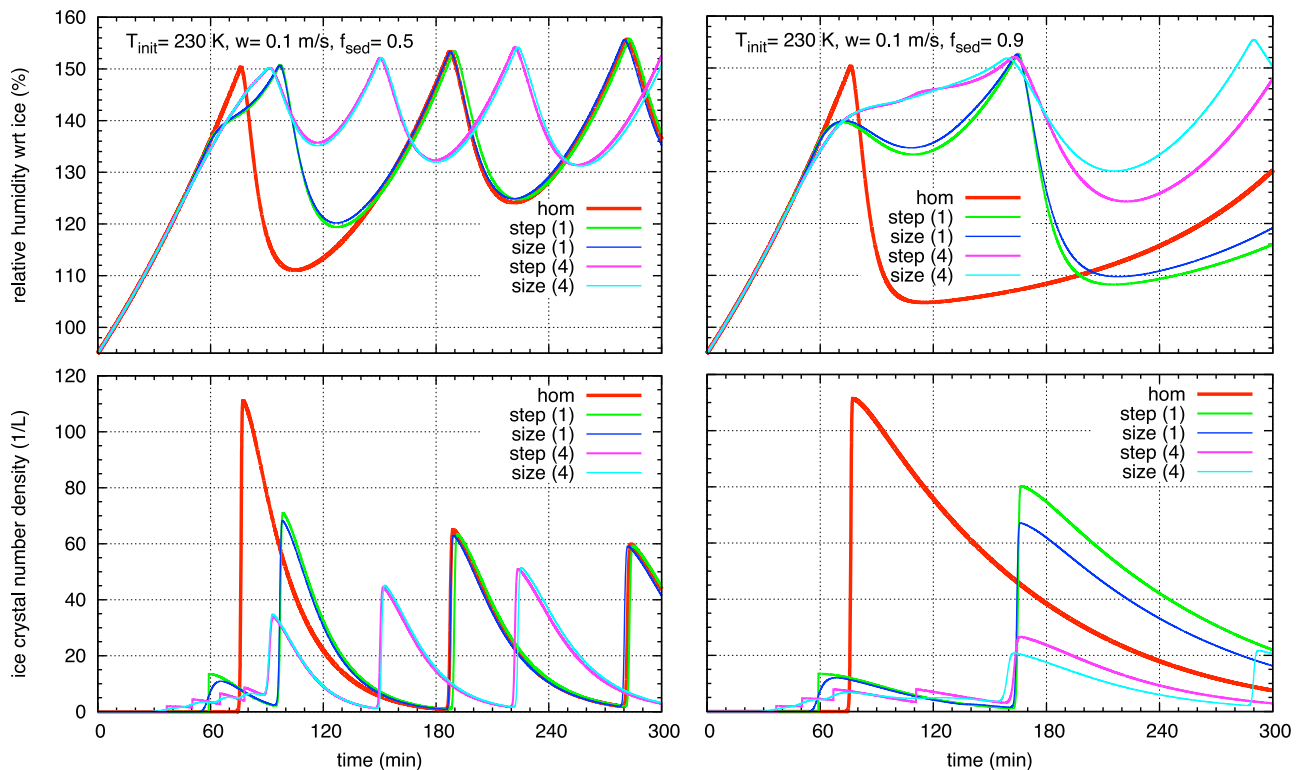


**Figure 6.** Two cases for determining the impact of heterogeneous nucleation on homogeneous nucleation for different experiments (“hom, step(1), size(1), step(4), size(4)”). The evolution of (top) relative humidity over ice (in %) and (bottom) ice crystal number density (in  $L^{-1}$ ) is shown for different values of the sedimentation flux ratio, (left)  $f_{sed} = 0.5$  and (right)  $f_{sed} = 0.9$ . For all experiments an initial temperature of  $T_{init} = 230$  K and a constant updraft of  $w = 0.1$  m  $s^{-1}$  is prescribed.

rate  $dRHi/dt$  is reduced over the entire time interval until homogeneous nucleation starts to form ice crystals at around  $t \sim 88$  min, however, at a quite low value producing a strongly reduced ice crystal number concentration.

[58] As in case of internally mixed IN there were marginal differences between experiments “step(4), size(4)”, mostly driven by the discrete nature of the step-wise parameterization. The ice crystal number density produced in the homogeneous nucleation event is quite similar in both cases but drastically reduced when compared to the reference experiment “hom”. Due to sedimentation of ice crystals the relative humidity increases again after the first homogeneous nucleation event, forming ice crystals at times  $t \sim 149, 220$  min, respectively.

[59] Another general feature of the modification of homogeneous nucleation events can be observed in experiments “step(4)/size(4)”. The ice crystal concentration, formed in subsequent homogeneous nucleation events, increases for each subsequent peak. For a longer simulation period it would be expected that in experiments including heterogeneous IN the peak would ultimately reach the same value as for the reference simulation “hom” after all heterogeneously formed ice crystals are fallen out. That is to say, after some time the experiments with heterogeneous IN should reach the same state as for pure homogeneous nucleation. In contrast, the preceding heterogeneous nucleation events seem to affect also subsequent homogeneous nucleation events. Although the heterogeneously formed ice crystals

have fallen out significantly earlier ( $n_{het} < 0.1$   $L^{-1}$  at  $t \sim 140$  min) due to changes in the relative humidity rate at some point the entire evolution of the rate is changed triggering a different behavior. The disturbed time evolution of  $RHi$  then affects the subsequent ice crystal number concentrations. This behavior is an important reason to include heterogeneous IN into studies and in comparisons of cloud lifetimes. More about this effect can be found in the discussion in section 5.

[60] For the scenario representing the middle of cloud ( $f_{sed} = 0.9$ ) the result changes (Figure 6, right, and Figure 7, bottom). The qualitative behavior for the experiments is outwardly similar except for a reduction of the sedimentation process, which crucially affects the competition or even balance between the relative humidity shaping processes (cooling, growth, sedimentation). Thus, ice crystal growth is more dominant, because ice crystals tend to remain longer in the box; heterogeneously formed ice crystals can have a stronger impact on the evolution of the relative humidity than in case representative for the cloud top. We again first consider the case of experiments “step(1)/size(1)”: Heterogeneous nucleation has its onset at about  $t \sim 60$  min. However, due to the longer residence of ice crystals in the box, ice crystal growth is strong enough to drive the rate  $dRHi/dt$  to negative values, i.e. the relative humidity is decreasing; it takes longer until positive terms of  $dRHi/dt$  (cooling and sedimentation) dominate the rate. Up to about  $t \sim 135$  min, the experiments “step(1)” and “size(1)” were

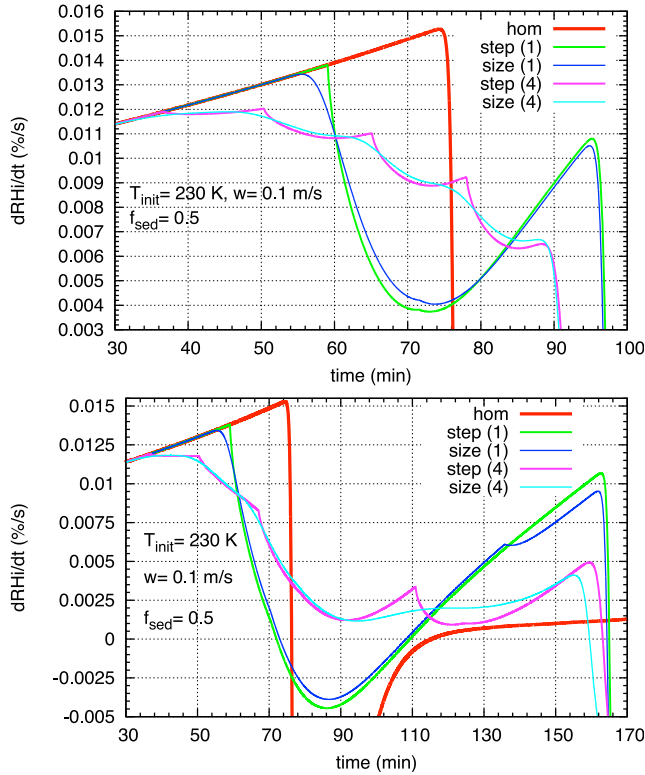


**Figure 7.** Rate  $dRHi/dt$  for the reference cases (top)  $f_{sed} = 0.5$  and (bottom)  $f_{sed} = 0.9$  and all parameterizations (“hom”, “step(1)/size(1)/step(4)/size(4)”). The evolution is shown up to the onset of homogeneous nucleation in experiments “step(1)/size(1)/step(4)/size(4)”. For all experiments an initial temperature of  $T_{init} = 230$  K and a constant updraft of  $w = 0.1$  m s<sup>-1</sup> is prescribed.

quite similar, except for the already noted difference of a more smooth rate for the size-dependent parameterization. Due to the size-dependent nucleation parameterization not all available IN were consumed in the first heterogeneous nucleation event (starting at  $t \sim 55$  min), thus as the relative humidity increases further, the rest of the available IN nucleate in a secondary event, forming a tiny additional amount of  $\Delta n_c \sim 0.6$  L<sup>-1</sup>. However, because of the almost non-existent sedimentation, this additional amount of ice crystals changes the relative humidity rate leading to a slightly different peak rate at  $t \sim 165$  min, when a homogeneous nucleation event was triggered (see Figure 7, bottom). In comparison to the reference case (“hom”) a time shift can again be observed, the homogeneous nucleation event is shifted to a later time but the strength is almost the same as in case of pure homogeneous nucleation.

[61] Strong differences between experiments representing internally mixed (“step(1)/size(1)”) versus externally mixed (“step(4)/size(4)”) IN are observed; generally, externally mixed IN have a more pronounced impact on the evolution of  $RHi$  and the change in homogeneously formed ice crystal number concentrations compared to the reference simulation (“hom”). The impact of size, represented by experiments “size(1)/size(4)” seems to be less important. However, the impact of size-dependent versus step-wise parameterizations for externally mixed IN is more pronounced in simu-

lations representative for the middle of the cloud ( $f_{sed} = 0.9$ ). Although the main structure of the time evolution of  $RHi$  is quite similar for all simulations, small changes in key processes growth and sedimentation by preexisting heterogeneously formed ice crystals lead to strong changes, as can be seen clearly in the rate  $dRHi/dt$  (see Figure 7, bottom). In a short summary, we can conclude from these experiments that the difference between internally versus externally mixed IN is much more pronounced than the differences between step-wise and size-dependent heterogeneous nucleation. More precisely, we can state as follows: (1) Heterogeneous IN do influence subsequent homogeneous nucleation events, i.e. they affect the relative humidity and its rate  $dRHi/dt$ . (2) This influence can result into a shift in the subsequent homogeneous nucleation event and/or into a reduction of subsequent homogeneous nucleation events; the nucleation events “recover” until they have reached the same strength as in the undisturbed case after some time. (3) The different behavior of internally versus externally mixed IN is often more important than size-dependent nucleation thresholds. (4) Size effects become more important if heterogeneously formed ice crystals stay longer in the cloud layer ( $f_{sed} = 0.9$ , representing the middle of a cloud); in such cases the impact of heterogeneous IN is generally more pronounced.

### 4.3. Impact of Temperature and Updraft Changes

[62] In section 4.2 we have described the main features of the impact of heterogeneous IN on homogeneous nucleation events. However, the question arises how this qualitative picture changes for different environmental conditions such as temperature and vertical updrafts. For this purpose we have carried out a set of simulations for variable initial conditions, i.e.  $T_{init} = 210/220/230/240$  K,  $w = 0.05/0.1/0.15/0.2$  m s<sup>-1</sup>,  $f_{sed} = 0.5/0.9$  as indicated in section 3.

[63] In general, a gradual transition in importance of including size-dependence and/or external mixtures of IN was observed. For warm temperatures and/or low vertical velocities there were strong differences between step-wise and size-dependent parameterizations as well as between internally and externally mixed IN in terms of influencing subsequent homogeneous nucleation events and the formed ice crystal number concentrations. By decreasing temperature and/or increasing vertical velocity size became less important and internally versus externally mixtures becomes the more important factor. Proceeding further (yet lower temperatures/higher vertical velocities), the differences between the parameterizations vanish completely and only the existence of heterogeneous IN is important. There is an additional dependence on the sedimentation as stated above, indicating a more pronounced impact of size-dependent parameterizations in regimes with less net sedimentation, as mentioned in section 4.2.

[64] We have summarized this transition for the simulations in Tables 3 and 4, qualitatively. The entry “size” marks simulations where differences between all parameterizations were observed, i.e., the size information induces additional differences due to the number of IN types. The entry “num” marks simulations where only the number of treated aerosols produced a difference. Finally, the entry “no” indicates simulations where the differences between the different parameterizations vanished.

**Table 3.** Sensitivity of Simulations With  $f_{sed} = 0.5$  Due To Temperature and Vertical Velocity<sup>a</sup>

$f_{sed} = 0.5$	240 K	230 K	220 K	210 K
0.05 m s <sup>-1</sup>	size	num/size	num	no/num
0.10 m s <sup>-1</sup>	size	num	no	no
0.15 m s <sup>-1</sup>	size	no/num	no	no
0.20 m s <sup>-1</sup>	num/size	no/num	no	no

<sup>a</sup>Here “no” indicates essentially no changes between using different IN parameterizations; “num” indicates changes between using different numbers of aerosol types; and “size” indicates additional differences resulting from the number of aerosol types by using additionally size-dependent parameterizations.

[65] We want to state here that *for all* these simulations there is an impact of heterogeneous IN on homogeneous nucleation when compared to the respective reference simulation “hom”. Figure 8 shows an example of the impact of heterogeneous nucleation for a simulation starting at  $T_{init} = 210$  K with an updraft of  $w = 0.1$  m s<sup>-1</sup>. Here, the ice crystal number concentration in experiment “size(4)” is strongly reduced compared to the reference case (“hom”). Changes in sedimentation factor do not crucially impact the time evolution as ice crystals remain quite small during the entire simulation because of a high concentration and less available water vapor at these cold temperatures. This makes clear that also for cold temperatures, homogeneous nucleation could be modified by heterogeneous IN.

[66] While Tables 3 and 4 gives a qualitative overview of the importance of different IN parameterizations, we have also tried to quantify this overall impact of heterogeneous IN on homogeneous nucleation. For this purpose we compare for each simulation series the maximum homogeneously formed ice crystal number concentration of the experiments “step(1)/size(1)/step(4)/size(4)” with the ice crystal number concentration formed in the reference simulation during the entire simulation time. This impact is quantified by the following formula:

$$r_{IN} = \frac{\max_{ex=step(1/4)/size(1/4)}(n_{hom,ex})}{\max n_{hom,hom}}. \quad (10)$$

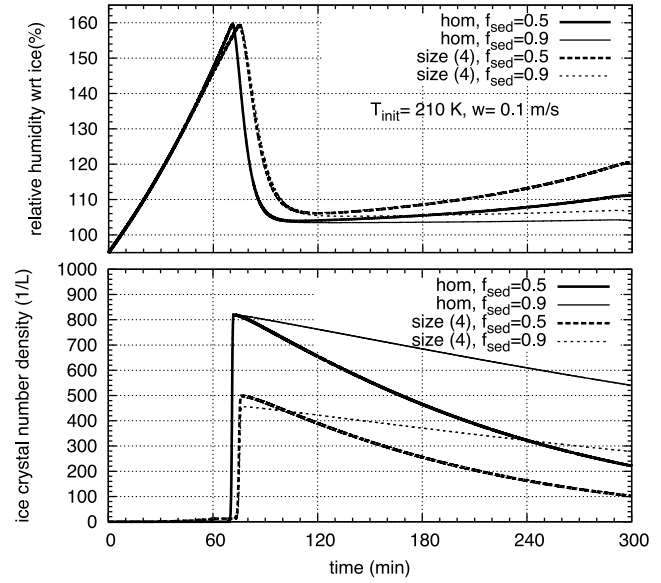
This quantity measures the overall reduction of homogeneously formed ice crystals by heterogeneous IN compared to the reference case without any heterogeneous IN.

[67] The overall impact of heterogeneous IN on the maximum ice crystal number concentration of homogeneously formed ice crystals is quite pronounced: The median value is

**Table 4.** Sensitivity of Simulations With  $f_{sed} = 0.9$  Due To Temperature and Vertical Velocity<sup>a</sup>

$f_{sed} = 0.9$	240 K	230 K	220 K	210 K
0.05 m s <sup>-1</sup>	size	size	num/size	num
0.10 m s <sup>-1</sup>	size	size	num	no
0.15 m s <sup>-1</sup>	size	num/size	no	no
0.20 m s <sup>-1</sup>	size	num	no	no

<sup>a</sup>Here “no” indicates essentially no changes between using different IN parameterizations; “num” indicates changes between using different numbers of aerosol types; and “size” indicates additional differences resulting from the number of aerosol types by using additionally size-dependent parameterizations.

**Figure 8.** (top) Relative humidity over ice (in %) and (bottom) ice crystal number concentration (in L<sup>-1</sup>) for simulations (experiments “hom” versus “size(4)”,  $f_{sed} = 0.5/0.9$ ) starting at  $T_{init} = 210$  K with a constant updraft of  $w = 0.1$  m s<sup>-1</sup>.

med ( $r_{IN}$ ) = 0.421, while the ratio is in the range  $0.044 \leq r_{IN} \leq 0.970$ ; thus, there is a strong reduction of the maximum ice crystal number concentration compared to experiment “hom”. As one would expect, the impact of heterogeneous IN is stronger in case of  $f_{sed} = 0.9$  than in case of  $f_{sed} = 0.5$ . For simulations representing the cloud top ( $f_{sed} = 0.5$ ) the value of  $r_{IN}$  is in the range  $0.323 \leq r_{IN} \leq 0.970$  with a median value of med ( $r_{IN}$ ) = 0.527. In case representative for the middle of a cloud ( $f_{sed} = 0.9$ ) the value of  $r_{IN}$  is in the range  $0.044 \leq r_{IN} \leq 0.821$  with a median value of med ( $r_{IN}$ ) = 0.1805. Thus, for a normal background concentration of available IN ( $\sim 10$  L<sup>-1</sup>), there is a general reduction in the maximum number concentration of homogeneously formed ice crystals compared to the undisturbed reference simulation “hom”.

[68] However, there is no clear signal indicating a dependence on parameterizations or vertical velocity. There is a weak indication that for low temperature the reduction of homogeneously formed ice crystals is more pronounced. Overall, this corroborates that the behavior of the relative humidity evolution is very sensitive and small changes can lead to very strong response in terms of homogeneous ice nucleation. Nevertheless, there is a slight indication that externally mixed IN (step-wise and size-dependent parameterizations, respectively) reduce the maximum ice crystal number concentration slightly more than internally mixed IN.

#### 4.4. Polluted Scenario

[69] Within this section we concentrate on a polluted scenario, i.e., a total background heterogeneous IN concentration of  $n_a = 140$  L<sup>-1</sup>, comparable to the measurements reported by DeMott *et al.* [2003b]. One would expect from earlier studies without sedimentation [e.g., Gierens, 2003] that heterogeneous IN could completely suppress homogeneous nucleation if heterogeneously formed ice crystals stay in the box for a long time. In fact, this is the case over the complete

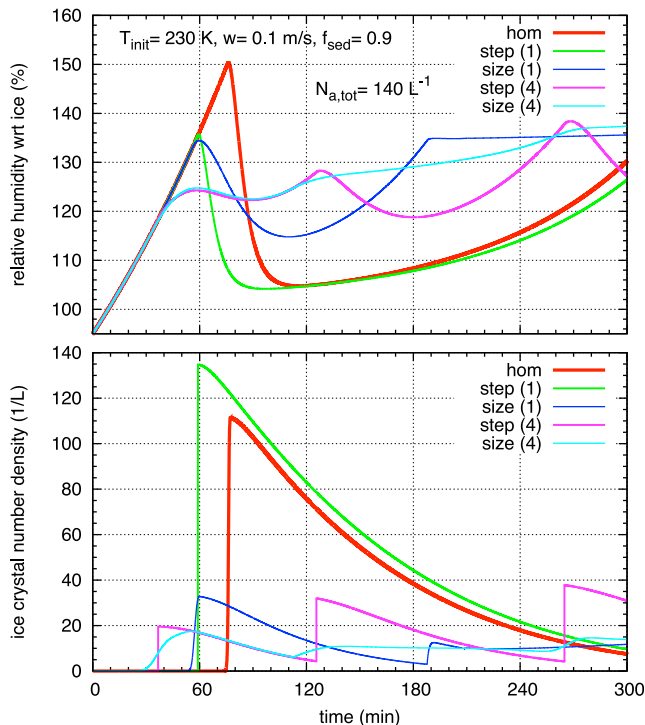
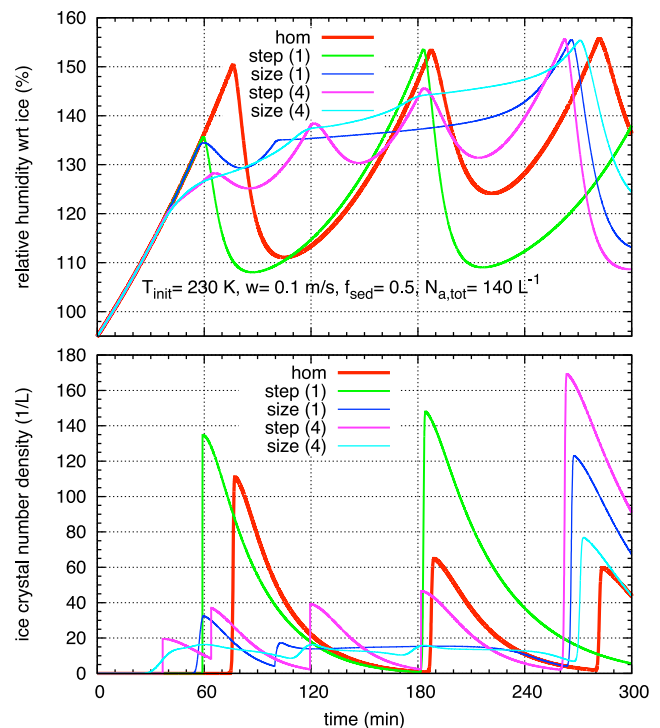


**Figure 9.** (top) Relative humidity over ice (in %) and (bottom) ice crystal number concentration (in L $^{-1}$ ) in experiments “hom, step(1), size(1), step(4), size(4)” for initial temperature  $T_{init} = 230$  K, a constant updraft of  $w = 0.1$  m s $^{-1}$  and a sedimentation factor of  $f_{sed} = 0.9$ ; here, a polluted background is assumed ( $n_a = 140$  L $^{-1}$ ).

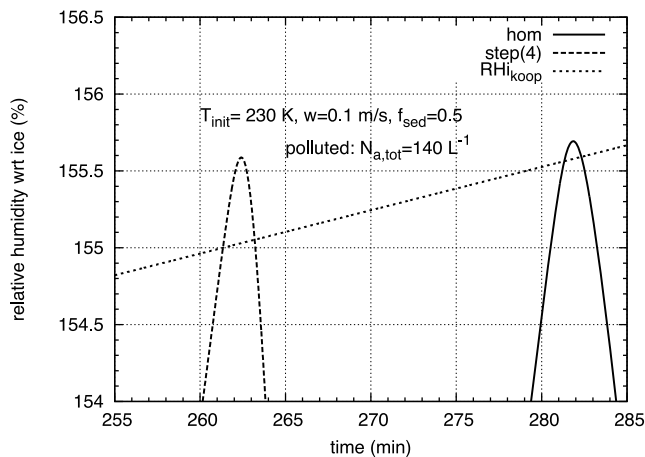
duration in (almost) all simulations with  $f_{sed} = 0.9$ . However, it can not be excluded that by progressing much further in time that in some cases homogeneous nucleation would eventually begin to form ice crystals. In Figure 9 a typical example of the impact of heterogeneous IN treated in the experiments “step(1)/size(1)/step(4)/size(4)” in comparisons to the homogeneous nucleation reference case “hom” is shown. For these simulations we again start with an initial temperature of  $T_{init} = 230$  K and a constant updraft of  $w = 0.1$  m s $^{-1}$ . The parameterizations produce very different amounts of ice crystals; here the size-dependent parameterizations differ significantly from the step-wise parameterizations, as expected. Note that the parameterization used in experiment “step(1)” behave similarly to homogeneous nucleation, i.e., (almost) instantaneously forming ice crystals. As stated above, laboratory measurements indicate a more size-dependent or even smooth behavior of heterogeneous nucleation [Archuleta *et al.*, 2005; Möhler *et al.*, 2006; Kanji and Abbatt, 2006]. Therefore this step-wise parameterization of heterogeneous nucleation seems to be a less physical description of the nucleation process. While for a normal background the differences between size-dependent and step-wise parameterizations are of lower importance, for a polluted background the differences are much larger and can lead to unphysical behavior, i.e. all available IN are activated at once. For simulations representing the cloud top ( $f_{sed} = 0.5$ ), heterogeneous IN do not completely switch off homogeneous nucleation. This is shown exemplarily in

Figure 10. Again, we start with an initial temperature of  $T_{init} = 230$  K and a constant updraft of  $w = 0.1$  m s $^{-1}$ . As expected, for large IN concentrations the impact of different parameterizations becomes more pronounced. While for the simulations with a normal background concentration the main difference was due to internal versus external mixtures of IN (i.e. one versus four classes of IN), in the polluted cases the impact of size-dependent parameterizations becomes more important. This can be seen clearly in Figure 10. Beneath the large differences in the simulations due to different parameterizations, it is obvious that in all cases first homogeneous nucleation is suppressed and just at the end of the simulation time homogeneous nucleation can finally produce ice crystals.

[70] An additional and quite contra-intuitive feature can be observed: Although homogeneous nucleation is suppressed in the first part of the simulations, at later times the amount of nucleated ice crystals is higher for the experiments including heterogeneous IN than for the reference simulation “hom”. The reason for this lies in subtle changes in the relative humidity rates due to the growth/sedimentation of heterogeneously formed ice crystals. These crystals change the shape of the humidity rate. An additional but minor factor is that the reservoir of the background aerosols for homogeneous freezing (i.e. sulfuric acid) is changed compared to the reference case; strong nucleation events lead to a decrease of the background aerosol, which is trapped in the formed ice crystals. This also changes the amount of homogeneously nucleated ice crystals, because the size distribution is changed to less and smaller sulfuric acid particles, thus less large solution droplets are available in the next freezing event. In Figure 11 it is shown how the



**Figure 10.** The same experimental conditions as in Figure 9 but for  $f_{sed} = 0.5$ .



**Figure 11.** Overshooting over the homogeneous nucleation threshold ( $RH_{i,koop}$ ) for solution droplets of size  $r_d = 0.25 \mu\text{m}$  for the simulations “ref” and “step(4)” for an initial temperature  $T_{init} = 230 \text{ K}$ , a constant updraft of  $w = 0.1 \text{ m s}^{-1}$  and a sedimentation parameter of  $f_{sed} = 0.5$ . The entire relative humidity evolution is shown in Figure 10.

overshooting of the relative humidity over the threshold for homogeneous nucleation  $RH_{i,hom}(T)$  (for solution droplets of size  $r_d = 0.25 \mu\text{m}$ ) differs between the reference case “ref” and the experiment “step(4)”. The shape of the peak is changed, the overshooting for experiment “step(4)” is higher and takes longer than for the reference simulation. As mentioned earlier, the overshooting determines the amount of nucleated ice crystals. In some cases not only the maximum value of the overshooting but also the width is changed. This feature can also lead to a different amount homogeneously formed ice crystals. It should be noted that in the reference case the later nucleation events are still disturbed by the ice crystals produced in earlier nucleation events, which stay in the box; they also change the relative humidity rates and therefore influence the following nucleation events.

[71] All different scenarios were also investigated for the polluted case ( $T_{init} = 210/220/230/240 \text{ K}$ ,  $w = 0.05/0.1/0.15/0.2 \text{ m s}^{-1}$ ). It turned out that in all cases the first potential homogeneous nucleation event is strongly suppressed. Homogeneous nucleation does not show up for  $f_{sed} = 0.9$  (middle of cloud) over the whole simulation time. For simulations representative for the cloud top ( $f_{sed} = 0.5$ ) in most cases there is a total reduction of the homogeneously formed ice crystal number concentration compared to the reference case “hom”. The reduction factor (compared to the reference case) is in the range  $0.0013 \leq r_{IN} \leq 0.986$  with a median value of  $\text{med}(r_{IN}) = 0.532$ . In some cases the phenomenon of a slight enhancement of the homogeneously formed ice crystal number concentration can be observed, as described above. This enhancement occurs only for low vertical velocities and/or high temperatures and preferably for step-wise parameterizations; however, this is maybe also an indication that for high IN concentrations a step-wise parameterization is maybe not an appropriate choice.

[72] A very short summary of the polluted cases, and increased IN in general, can be stated as follows: In all cases, no matter if homogeneous nucleation is suppressed

totally or not, the results depend very strongly on the parameterizations. Laboratory and field data would suggest that in most cases a size-dependent parameterization for all IN classes seems most appropriate to describe the heterogeneous nucleation process.

## 5. Discussion

[73] In all simulations we observe that a key mechanism leading to the modification of homogeneous nucleation by heterogeneous IN is the competition between the three relative humidity shaping processes: cooling, ice crystal growth and sedimentation. Because of the highly non-linear nature of these processes small changes in the environmental and cloud properties can ultimately have large impacts. While cooling is not affected by microphysics, of course, additional heterogeneously formed ice crystals influence the resulting  $RHi$  rate via growth and sedimentation. The influence of preexisting heterogeneous nucleation events is manifested in two general features, which are originating from the modification of the  $RHi$  time evolution.

[74] First, in some cases, the first homogeneous nucleation event after preexisting heterogeneous nucleation event(s) is very weak (i.e. only few ice crystals are formed). However, a kind of recovery can be observed in subsequent homogeneous nucleation events: The peak values of ice crystal concentrations are increasing until after some time the originally disturbed homogeneous nucleation events have the same strength as in the undisturbed case (“hom”). The time for the recovery can vary; in some cases it is very short (see Figure 6, left) but it could also last for the entire simulation time.

[75] Second, the change of  $RHi$  time evolution by growth and sedimentation of heterogeneously formed ice crystals lead to a time shift in nucleation events. A homogeneous nucleation event, which would occur in the undisturbed case (“hom”) is suppressed in case of additionally available heterogeneous IN, but it occurs at later time with an equal strength. Thus, the time evolution of forming ice crystals is just shifted by preexisting heterogeneous IN.

[76] These two effects, although looking quite different, origin from the same source, namely the change of the balance between the key processes (cooling, growth and sedimentation) determining the time evolution of  $RHi$  and the rate  $dRHi/dt$  by heterogeneously formed ice crystals.

[77] For an estimate of the importance of the modification of homogeneous nucleation these two effects must be considered. Generally, we can state that a change in the ice crystal number concentration in the range that we have observed in our simulations ( $0.044 \leq r_{IN} \leq 0.970$ ,  $\text{med}(r_{IN}) = 0.421$ , see section 4.3) has a strong impact on the cirrus cloud. If we change our perspective from microphysical details to a more general picture of cloud evolution, we can qualitatively estimate the importance of the two effects changing the cloud structures. Obviously, the first effect, changing the ice crystal number concentration over a longer time is more important. If the modification impact last for a longer time (i.e., it is not only present for the young cirrus) this could influence macro- and microphysical properties of the cloud and the environment. For instance, the radiation properties could be changed. From recent studies such as that by *Fusina et al.* [2007] we know that the transition

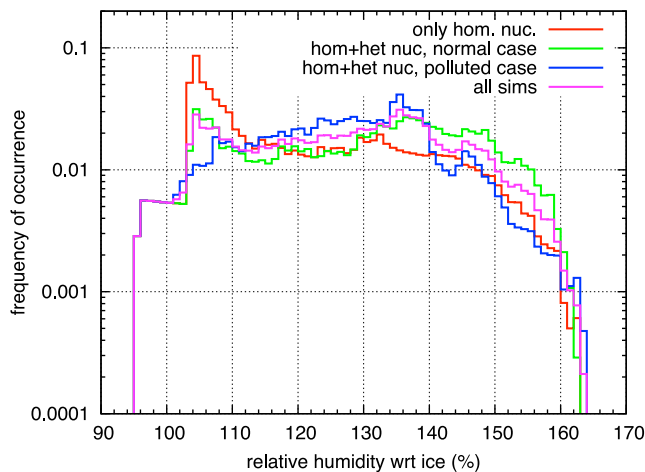


**Figure 12.** Frequency of occurrence of relative humidity over ice for only homogeneous nucleation (experiments “hom”, red line), for homogeneous/heterogeneous nucleation in a normal background (experiments “size/step(1/4)”, green line), for homogeneous/heterogeneous nucleation in a polluted background (experiments “size/step(1/4)”, blue line) and for all experiments together (all experiments, purple line).

between net warming and net cooling of a thin mid-latitude cirrus cloud depends crucially on the ice crystal number concentration, while ice water content mainly determine the strength of the warming/cooling. If the ice crystal number concentration is decreased by the impact of heterogeneous IN a stronger warming (or even a warming instead of a cooling) could result. Thus, if the modification prolongs the duration of this status of the cirrus this becomes increasingly important.

[78] By contrast, a pure phase displacement or time shift only rearranges the evolution of the relative humidity. Thus, after an initial period where its properties have changed the cirrus layer has, more or less, the same properties in terms of ice crystal number concentration. However, this could lead to a different physical location where the cloud forms: If we assume a mean horizontal velocity of  $u \sim 10 \text{ m s}^{-1}$  and a ‘typical’ phase displacement of  $\Delta t \sim 30\text{--}60 \text{ min}$ , a shift of location in an order of 20–40 km could be possible. This could be maybe important for investigations on a regional scale. Generally, it would be difficult to attribute such changes in occurrence of cirrus clouds to this microphysical effect using measurements. Such changes could either be masked by dynamics or even assumed to be determined by variations in meteorology. An additional complication for estimating these effects at least is the different behavior of the cirrus layers according to their sedimentation properties. For instance, it could happen that for the top layer with  $f_{sed} = 0.5$  the impact of modification is marginal, whereas for the layer in the middle of the cloud ( $f_{sed} = 0.9$ ) the modification is much stronger (see, e.g., Figure 6). All these questions can also be placed in the context of contrail–cirrus. Indeed, a spreading contrail is an additional supersaturation sink and the question again arises how this modification of the competition of cloud processes would influence a possible later homogeneous nucleation event.

[79] In an additional step we have investigated statistically the relative humidity which occurs in our simulations (Figure 12). In the RH*i* statistics it can be seen clearly, that high ice supersaturation in the range between 100% and the homogeneous nucleation thresholds can occur. It is obvious from looking at the time evolution of relative humidity that in many cases there is no relaxation of the relative humidity to values near saturation, as often claimed [see, e.g., Hoyle *et al.*, 2005]; the main cause for this is the permitted sedimentation, which removes the supersaturation sink (i.e. the ice crystals) inside the box. However, the behavior is strongly dependent on the environmental conditions: For colder temperatures and/or higher vertical velocities, the relaxation to values near saturation can be observed due to the large amount of ice crystals formed by homogeneous nucleation.

[80] These results are consistent with results from single column models [Kärcher, 2005; Comstock *et al.*, 2008] and cloud-resolving models [Spichtinger and Gierens, 2009b, 2009c]. Thus, at least for the moderate temperature range  $210 \leq T \leq 240 \text{ K}$  (i.e. for mid latitude conditions) the occurrence of high ice supersaturation inside cirrus clouds might partly be explained by competition of homogeneous/heterogeneous nucleation within the same environment [see also Spichtinger and Gierens, 2009c]. It should be noted, that there were no significant qualitative differences in the RH*i* statistics for normal versus polluted background IN concentrations.

[81] Finally, we want to mention that the probable increase of the total aerosol burden within the next 50 to 100 years [Stier *et al.*, 2006] might enhance the number concentration of aerosols and possibly also the number concentration of available IN. Thus, the “polluted” scenarios could become more important in future, leading possibly to different cirrus cloud properties than today.

[82] In our investigation we focus on “mostly comparable” parameterizations, i.e. we choose the thresholds for the heterogeneous IN such that (a) the average value of relative humidity over ice where nucleation starts is around 130–135% and (b) for external mixtures the “better” IN (i.e. activated at low RH*i* values) are less numerous. However, one could ask the question, how our results would change if all IN are concentrated in a class of “good IN”, i.e. the activation threshold is very low. We have run some sensitivity simulations to check this question. To be precise, we have run two different classes of simulations for the normal background IN concentration ( $n_{a,total} = 14 \text{ L}^{-1}$ ) of internally mixed IN (only one class of ice/aerosols) for the whole parameter space of initial temperature (210/220/230/240 K) and constant updrafts (0.05/0.1/0.15/0.2  $\text{m s}^{-1}$ ), respectively. For the first class of simulations we use a step-wise parameterization with a humidity threshold of  $RHi_{het} = 118.3\%$ ; for the second class of simulations we choose a size-dependent parameterization corresponding to the low step-wise humidity threshold as mentioned above (see parameterization size(4), type 1 in Table 1 and Figure 2, respectively). It was observed that due to the earlier start of heterogeneous nucleation (lower nucleation threshold compared to standard simulations) the time evolution of the RH*i* is changed. However, while for the cloud top layer ( $f_{sed} = 0.5$ ) the earlier onset of heterogeneous nucleation

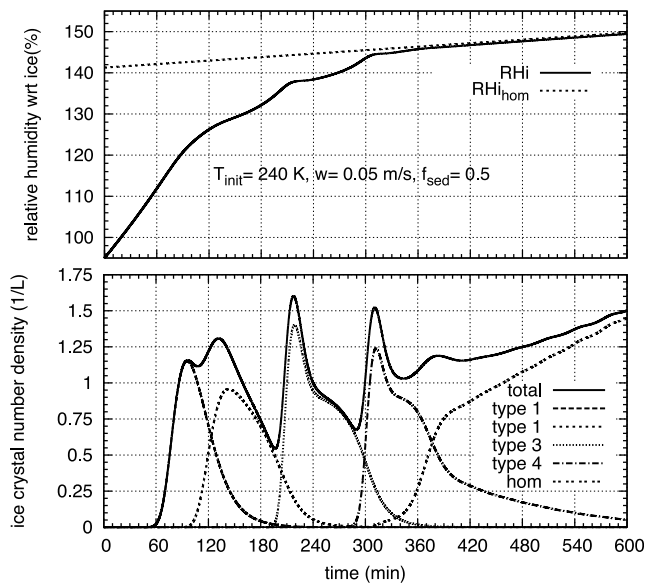


**Figure 13.** (top) Relative humidity over ice (in %) and (bottom) ice crystal number densities (in  $L^{-1}$ ) for a cooling event ( $w = 0.05$ ) starting at  $T_{init} = 240$  K. IN parameterization “size(4)” is used with a less pronounced sedimentation, i.e.  $f_{sed} = 0.9$ . This case is meant to mimic a subvisible cirrus, which is not in equilibrium. For comparisons, the evolution of a representative threshold for homogeneous freezing of solution droplets of a distinct size is included in Figure 13 (top) (dotted line).

leads to a shift in the onset of homogeneous freezing (compared to the experiments “ref” as well as “step(1)” and “size(1)”), the ice crystal number concentration formed in homogeneous nucleation events does not change strongly compared to the former simulations “step(1)/size(1)”. In simulations representative for the middle of a cloud ( $f_{sed} = 0.9$ ), the differences between the simulations become larger; however, the differences in homogeneously formed ice crystal number concentrations between the different simulations including heterogeneous nucleation remains quite small. Thus, more effective IN can change the time evolution of relative humidity over ice and introduce different time shifts, however the qualitative behavior and the amount of homogeneously formed ice crystals is not changed drastically compared to the simulations before.

[83] Finally, but not of least importance, we present a special case indicating that homogeneous nucleation is not necessarily an almost step-wise process. This was the case for the simulation starting with  $T_{init} = 240$  K and a moderate updraft velocity of  $w = 0.05$  m  $s^{-1}$ . The further assumptions were a normal background aerosol concentration, a layer in the middle of a cloud ( $f_{sed} = 0.9$ ) and IN parameterization of “size(4)”. In Figure 13 the evolution of the relative humidity (Figure 13, top) and the successively nucleated ice crystal number concentration (Figure 13, bottom) are shown, respectively. It can be seen that ice crystals nucleate heterogeneously from all four classes. The formed ice crystals do not significantly reduce the supersaturation. Thus, at around  $t = 300$  min, homogeneous nucleation starts but not as usual with a pronounced overshoot but more in an asymptotic behavior approximating homogeneous nucle-

ation thresholds. Just enough ice crystals are formed to allow the relative humidity to remain close to the homogeneous nucleation threshold. It is interesting to note that compositional differences among the particles that homogeneously freeze have been observed [Cziczo *et al.*, 2004b]. Thus, homogeneous nucleation of this sort could lead to preferential sedimentation of certain aerosol types as is observed for heterogeneous nucleation. This cirrus is not in equilibrium and, due to the small amount of ice crystals, it would probably be considered a subvisible cirrus. This case is related to the formation of subvisible cirrus by purely homogeneous nucleation as described by Kärcher [2002].

## 6. Summary and Conclusions

[84] In this study we have investigated the impact of heterogeneous IN on subsequent homogeneous nucleation events. For this purpose we have extended an existing ice microphysics scheme with a new approach for considering sedimentation within the framework of a box model. Further, we have developed and implemented a new size-dependent parameterization for heterogeneous nucleation. The sedimentation approach and the nucleation parameterization were used for a series of box model simulations considering the modification of homogeneous nucleation by heterogeneously formed ice crystals.

[85] Instead of investigating asymptotic time scales (as, e.g., in work by Gierens [2003] and Kay *et al.* [2006]) we evaluate the actual relative humidity rate  $dRH_i/dt$ . This allows us to investigate the impact of the three different competing processes, namely adiabatic cooling, growth and sedimentation, shaping the time evolution of relative humidity. While the general finding that heterogeneous nucleation can impact homogeneous freezing events is not totally new, we investigate this impact from a new point of view in more details using the relative humidity rate.

[86] A major outcome of the study is that for the environmental conditions used in the setup (constant updraft in the range of  $0.05 \leq w \leq 0.2$  m  $s^{-1}$ , initial temperature  $T_{init} = 210/220/230/240$  K) heterogeneous IN always have an impact on the following homogeneous freezing events. The general influence can be determined as the change of the relative humidity rate due to additional cloud condensate inside the box leading to a different behavior due to the processes growth and sedimentation, respectively. This main impact on the relative humidity time evolution and the relative humidity rate leads to a weakening of a following homogeneous nucleation event, i.e. it results into a reduction of homogeneously formed ice crystal number concentration compared to the undisturbed case. This general effect can lead to two different effects in the time evolution of the cloud.

[87] 1. Time shift/Phase change: Heterogeneous nucleation at earlier times in the simulation (compared to the reference simulation with pure homogeneous nucleation) causes a delay or time shift for the following homogeneous nucleation events (i.e. it takes place later). This shift can be continued over the whole simulation, i.e. although the same strength of a homogeneous nucleation event is ultimately reached, the event is shifted compared to the reference simulation.

[88] 2. Delayed recovery of nucleation events: Heterogeneous nucleation reduces the first subsequent homogeneous nucleation event; however, due to the change in the rate by this new event the time evolution of  $RHi$  is disturbed. The following homogeneous nucleation events grow with time, until they reach a strength comparable to the events in the reference simulation.

[89] A major new outcome of this study is the impact of internal versus external mixtures of IN, which turns out to be important. The time evolution of relative humidity and thus the homogeneous nucleation events depend strongly on this property of IN. The impact of internal versus external mixtures depends on the environmental conditions (temperature and updraft) and becomes more important for warmer temperatures and/or lower vertical velocities. The differences between the impact of internal and external mixtures on homogeneous nucleation events increases drastically for a polluted background (total IN concentration  $140 \text{ L}^{-1}$ ) compared to a “normal” background (total IN concentration  $14 \text{ L}^{-1}$ ).

[90] If we additionally take into account size-dependent nucleation thresholds the picture changes again. In some cases, a size-dependent nucleation threshold for heterogeneous nucleation introduces differences compared to the “step-wise” parameters. This is again strongly dependent on environmental conditions (temperature and updraft) and it can be stated that size-dependent parameterizations are more important for warmer temperatures and/or lower vertical velocities. Additionally, in case of a polluted background a size dependent parameterization introduces a more realistic behavior of the nucleation event (i.e. a finite nucleation time) in contrast to the step-wise parameterizations. However, for low IN concentration, a step-wise parameterization is still appropriate. These findings have not been shown in earlier studies.

[91] Due to our new sedimentation parameterization, we are able to attribute simulations with different prescribed sedimentation flux ratios  $f_{sed} = 0.5/0.9$  as representative for different parts of synoptically driven cirrus clouds. Thus, in our approach the impact of heterogeneous IN on cloud formation and evolution in different cloud regimes can be investigated. Here, for the first time it is stated that box model studies are valid but only for a distinct region in the cloud; this is in contrast to former box model studies, which claims a kind of universality [e.g., *Haag and Kärcher, 2004; Kay et al., 2006, 2007*]. From the simulations we can conclude that the impact of heterogeneous IN is more pronounced in “sedimentation dominated” regions (middle of cloud), i.e. for  $f_{sed} = 0.9$ ; more heterogeneously formed ice crystals can stay longer in the box influencing the relative humidity rate by more pronounced growth and less important sedimentation. Thus, in these regimes, suppression of homogeneous freezing events is more probable; this is in agreement with studies which do not allow sedimentation [e.g., *Gierens, 2003*]. In regions with less sedimentation flux from above ( $f_{sed} = 0.5$ , i.e. cloud top) the impact of heterogeneous IN is less important.

[92] If one is only interested in the maximum amount of ice crystals formed during the whole simulation time, a surprising feature shows up: Only for cold temperatures and/or high vertical updrafts is there a significant reduction in the maximum number concentration compared to the reference

simulation. For warmer temperatures, the difference is vanishing or sometimes slightly higher ice crystal number concentrations are observed. This is due to subtle changes in the humidity rate and, in some cases, also due to the occurrence of the nucleation events at different temperatures.

[93] Last, but not least, the relative humidity statistics over all simulations show that competition between heterogeneous and homogeneous nucleation within the same environment can enhance the frequency of occurrence of high ice supersaturation (in the range  $100 \leq RHi \leq 165\%$ ) inside cirrus clouds. This result is consistent with former studies on the competition between heterogeneous and homogeneous nucleation in a cloud-resolving model [*Spichtinger and Gierens, 2009c*]. These findings indicate a possible explanation of high ice supersaturation inside cirrus under certain mid latitude environmental conditions. Additionally, we can cautiously conclude from our idealized model study that the impact of heterogeneous nucleation on following homogeneous nucleation events is probably most important for mid latitude conditions at higher temperatures and lower vertical velocities (e.g. in frontal cirrus clouds).

[94] We conclude this study with some recommendations for modelers and as experimentalists.

[95] 1. Recommendation for modelers: It is important to include heterogeneous nucleation into an ice microphysics scheme, including explicit aerosol impacts and washout. For some scenarios a more complex approach (size-dependent parameterization) is needed while for some cases the existence of several different aerosol classes is required (externally mixed IN). This effort is only worth using with a physically based homogeneous nucleation scheme [e.g., *Kärcher et al., 2006; Liu et al., 2007; Barahona and Neñes, 2008*].

[96] 2. Recommendations for experimentalists: The number density of IN is critically important in understanding cirrus cloud formation. Additionally, the relative humidity thresholds for heterogeneous nucleation of various aerosol types (mineral dust, soot, organics etc.) need to be better characterized; also their possible temperature dependence should be investigated. Finally, the effect of size on nucleation needs to be studied in greater detail.

[97] With the future development of more capable models the need for more, and more accurate, measurements of freezing properties of aerosols will become increasing evident. This problem could be solved by an enhanced use of IN counters on aircraft platforms as well as laboratory measurements [e.g., *Rogers et al., 2001; Stetzer et al., 2008*]. On the modeling side, the existing parameterizations have to be improved, including the issue of evaporation of ice crystals formed by a distinct IN class as well as aerosol processing inside ice crystals.

## Appendix A: Relative Humidity Rates—Sources and Sinks

[98] The structure of the different processes of cooling, growth and sedimentation changing the relative humidity can be seen by an analytical derivation. From the definition of the relative humidity we can write:

$$RHi = \frac{p \cdot q}{\epsilon \cdot e_i(T)} \quad (\text{A1})$$

where  $\epsilon = R_g/R_v$  denotes the ratio of the ideal gas constant for dry air and water vapor, respectively.  $e_i(T)$  denotes the saturation pressure of water vapor over ice. For the time derivative of  $RHi$  we can write

$$\frac{dRHi}{dt} = \frac{q}{\epsilon} \frac{d}{dt} \left( \frac{p}{e_i(T)} \right) + \frac{p}{\epsilon e_i(T)} \frac{dq}{dt} \quad (\text{A2})$$

In a first approximation we neglect latent heat release during the growth process; this is valid due to small cloud ice mixing ratios leading to small temperature changes and the approach of a box without interaction with its environment. Thus, the first term represents the rate driven by adiabatic cooling while the second part represents the rate driven by growth and sedimentation. Due to the usually small cloud ice mixing ratio this approximation is valid. In the following we only consider the second term, while the first term was derived previously [see, e.g., *Kärcher and Lohmann, 2002; Gierens, 2003*]. By introducing the cloud ice mixing ratio  $q_c$ , it follows that  $dq/dt = -dq_c/dt$ . For the description of the cloud mixing ratio we use the ansatz via an arbitrary ice crystal mass distribution  $f(m)$ .

[99] The distribution is normalized to the total ice crystal number concentration  $N_c$ , i.e.,  $\int f(m)dm = N_c$  or equivalently,  $f(m) = N_c \cdot g(m)$  with  $\int g(m)dm = 1$ . Thus the cloud ice mixing ratio is represented by:

$$q_c := \int_0^\infty f(m)mdm = N_c \cdot \int_0^\infty g(m)mdm \quad (\text{A3})$$

Now we derive an expression for  $dq_c/dt$ :

$$\begin{aligned} \frac{dq_c}{dt} &= \frac{d}{dt} \int_0^\infty f(m)mdm = \frac{d}{dt} N_c \cdot \int_0^\infty g(m)mdm \\ &= \frac{1}{N_c} \frac{dN_c}{dt} N_c \int_0^\infty g(m)mdm + \frac{d}{dt} \int_0^\infty f(m)mdm \\ &= \frac{q_c}{N_c} \frac{dN_c}{dt} + \frac{d}{dt} \int_0^\infty f(m)mdm \end{aligned} \quad (\text{A4})$$

The first term describes the rate of the number concentration driven by sedimentation because  $N_c$  does not change for pure growth. The second term contains the mass rate by growth and sedimentation and can be written as follow, using the continuity equation in mass-space [see *Spichtinger and Gierens, 2009a*, equation (40)]:

$$\frac{d}{dt} \int_0^\infty f(m)mdm = \int_0^\infty f(m) \frac{dm}{dt} dm \quad (\text{A5})$$

Here, we could interpret  $dm/dt$  as the advection velocity in the mass-space, split into two different processes:

$$\frac{dm}{dt} = \left. \frac{dm}{dt} \right|_{\text{growth}} + \left. \frac{dm}{dt} \right|_{\text{sedimentation}} \quad (\text{A6})$$

where  $dm/dt|_{\text{growth}}$  is described by the growth equation for the mass rate of a single ice crystal [see, e.g., *Stephens, 1983*, equation (1)]. In the following the different contributions are marked by subscripts “g” and “s”, respec-

tively. We end with the following contributions for the rate of cloud mixing ratio:

$$\frac{dq_c}{dt} = \underbrace{\frac{q_c}{N_c} \frac{dN_c}{dt}}_{\text{sedimentation}} + \underbrace{\int_0^\infty f(m) \frac{dm}{dt} \Big|_s dm}_{\text{sedimentation}} + \underbrace{\int_0^\infty f(m) \frac{dm}{dt} \Big|_g dm}_{\text{growth}} \quad (\text{A7})$$

and this translates to the different contributions for the relative humidity rate:

$$\frac{dRHi}{dt} = \underbrace{\left. \frac{dRHi}{dt} \right|_c}_{>0} + \underbrace{\left. \frac{dRHi}{dt} \right|_g}_{<0} + \underbrace{\left. \frac{dRHi}{dt} \right|_s}_{>0} \quad (\text{A8})$$

where the subscripts “c, g, s” denote contributions of processes cooling, growth and sedimentation, respectively. Note that the rates representing processes growth and sedimentation are coupled to each other while the cooling rate is only dependent on the vertical velocity. The rate representing the sedimentation of ice crystals is positive only if there is a net loss of ice crystals, or in other words only if  $f_{\text{sed}} < 1$ .

## Appendix B: Comparisons of Sedimentation Schemes in Box Models

[100] While in some earlier box model studies sedimentation was included [*Haag and Kärcher, 2004; Kay et al., 2006*], we compare here these schemes with our ansatz. In the studies mentioned above the flux through the top of the box is always neglected, i.e. the loss of mass/number concentration is determined by:

$$\psi(t_n) = \psi(t_{n-1}) \cdot \exp(-\alpha_\psi), \quad \alpha_\psi = \frac{v_\psi \cdot \Delta t}{\Delta z} \quad (\text{B1})$$

Therefore, a change in the sedimentation rates can only be achieved in changing the physical depth of the box  $\Delta z$ . Usually, the depth is set to  $\Delta z = 100$  m for strong impact of sedimentation and to values  $\Delta z = 500$ – $1000$  m for less impact of sedimentation. However, our approach is comparable to this assumption. For a quantitative comparison we set:

$$\psi' = \psi \exp(-\alpha_1); \quad \alpha_1 := \frac{v_\psi \Delta t}{\Delta z_1} \quad (\text{B2})$$

$$\tilde{\psi}' = \psi(f + (1-f) \exp(-\alpha_2)); \quad \alpha_2 := \frac{v_\psi \Delta t}{\Delta z_2} \quad (\text{B3})$$

Whereas equation (B2) is used in former studies [e.g., *Haag and Kärcher, 2004; Kay et al., 2006*] and equation (B3) represent our approach (see equation (4)). The subsequent time level is indicated by primes. Assuming  $\psi' \equiv \tilde{\psi}'$  we end up with the following identity:

$$\alpha_1 = \alpha_2(1-f) \quad (\text{B4})$$

or in terms of thickness of the box/layer:

$$\Delta z_1 = \frac{\Delta z_2}{1-f} \quad (\text{B5})$$

**Table B1.** Values of  $f_{sed}$  and  $\Delta z_1$  for Different But Comparable Sedimentation Parameterizations Assuming a Constant Value of  $\Delta z_2 = 50$  m

$f_{sed}$	$\Delta z_1$ (m)	Comment	Representative Cloud Region
0.5	100	as in work of <i>Kay et al.</i> [2006]	cloud top
0.9	500	as in work of <i>Kay et al.</i> [2006]	middle of cloud
0.95	1000	as in work of <i>Kay et al.</i> [2006] and <i>Haag and Kärcher</i> [2004]	middle of cloud

In this derivation we used the approximation  $\exp(-x) \approx 1 - x$  which is valid for  $x \ll 1$ .

[101] Thus, our approach of a fixed layer thickness but a variable flux ratio  $f_{sed}$  is principally equivalent to the use of a variable layer thickness without a flux through the top of the box as used in sedimentation parameterization in former studies. In Table B1 typical values for  $f_{sed}$  with a fixed layer thickness  $\Delta z = 50$  m are shown in Table B1.

[102] It should be noted that although the two approaches lead to the same results there is a conceptual advantage of our approach. This new sedimentation scheme is based on cloud resolving simulations where the sedimentation flux ratio can be calculated from the whole 2D simulations [*Spichtinger and Gierens*, 2009a, 2009b, 2009c], thus the assumption of a distinct value of  $f_{sed}$  has a sound basis. From these simulations we can also deduce that by prescribing a certain value of  $f_{sed}$  the box model simulations are only representative for a distinct part of the cloud. Additionally, our microphysics scheme was developed for small grid resolutions with vertical layers in order of  $\sim 10$ – $100$  m. Thus, prescribing a fixed layer depth is more appropriate than changing the whole thickness of the box model in order to obtain different sedimentation effects. We also note that some new studies on more dynamical regimes (e.g., orographic cirrus clouds [see *Joos et al.*, 2009]) indicate that the choice of a very thick and homogeneous cirrus cloud layer (as, e.g., in work by *Kay et al.* [2007]) is inappropriate, thus, small layers must be chosen for box model studies in such an environment. Last, but not least, our approach could be extended to different values of  $f_{sed}$  for mass and number concentrations and to time-dependent  $f_{sed}$ , i.e. the structure of the cloud layer could change in time.

### Appendix C: A “Realistic” Case

[103] In order to show the representativity of the idealized setups and simulations we finally show a “realistic” case. We use data of mineral dust IN published by *Archuleta et al.* [2005] and *Welti et al.* [2009] to construct a ‘realistic’ parameterization of (1) a mixture of different mineral dust IN and (2) an internally mixed “mean” mineral dust IN. In both cases we specify size-dependent freezing thresholds as well as step-wise freezing parameterizations in order to determine the impact of externally versus internally mixed IN and the impact of the size of IN. The parameterizations are represented in Figure C1. In the following, ‘step<sub>MD</sub>(1)’ and ‘size<sub>MD</sub>(1)’ denote experiments using IN type ‘mean’ in Figure C1, while ‘step<sub>MD</sub>(2)’ and ‘size<sub>MD</sub>(2)’ denote experiments using IN types 1 (Welti) and 2 (Archuleta) together with homogeneous nucleation. Note here, that in the ‘realistic’ case the IN parameterizations are quite close in terms of

the RHI-thresholds; this can be seen clearly for the step-wise parameterization. The fixed thresholds are within a narrow range (109–126.4%RH<sub>i</sub>). Thus, we expect a less pronounced difference between simulations using different parameterizations compared to the idealized setups, where the range for the thresholds is much broader (118.3–145.0% RH<sub>i</sub>). As in the idealized setups we initialize a total amount of IN concentrations of  $14 \text{ L}^{-1}$ . In case of externally mixed IN (‘step/size<sub>MD</sub>(2)’) the IN number concentration is split: The number concentration of the ‘better’ IN (type 1 (Welti) in Figure C1) is set to  $5 \text{ L}^{-1}$  while the number concentration of the ‘bad’ IN (type 2 (Archuleta) in Figure C1) is set to  $9 \text{ L}^{-1}$ , mimicking the occurrence of less good IN and more ‘bad’ IN. For a polluted background, the number concentrations are multiplied by 10.

[104] In Figures C2 and C3 we show exemplarily the impact of externally versus internally mixed IN and the impact of a size-dependent parameterization. Figure C2 shows time evolution of relative humidity over ice and ice crystal number concentration for a normal IN background for a constant updraft of  $w = 0.1 \text{ m s}^{-1}$  for initial conditions  $T_{init} = 230 \text{ K}$ ,  $p_{init} = 300 \text{ hPa}$  and sedimentation factors  $f_{sed} = 0.5/0.9$ , respectively. In Figure C3 the same as shown for the polluted case. First, we investigate the normal background case. It can be seen, that heterogeneous IN have again a strong impact on the evolution of RHI. The timeshift as explained above can be seen clearly. However, the differences between the different parameterizations are not that pronounced as in the idealized cases. This is mainly due to the fact that the parameterizations are quite close in terms of freezing thresholds, thus differences in the evolution of RHI remain small. Additionally, we could only use two classes of IN types due to lack of data. This additionally decreases the differences in nucleation and growth, respectively. While there is still a (small) difference between externally and internally mixed IN simulations, consistent with our findings above, there is hardly any difference between step-wise and size-dependent nucleation parameterizations for a normal IN background. Qualitatively the same behavior is seen for other vertical updrafts and initial temperatures (not shown). From this we can conclude, that in normal back-

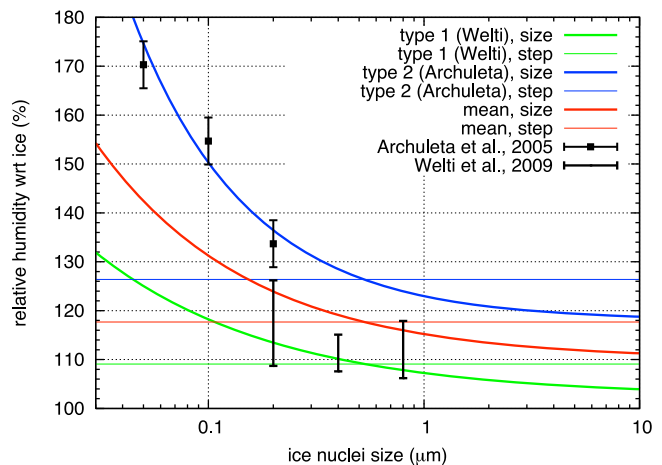


**Figure C1.** Freezing thresholds for a “realistic” case of mineral dust ice nuclei.

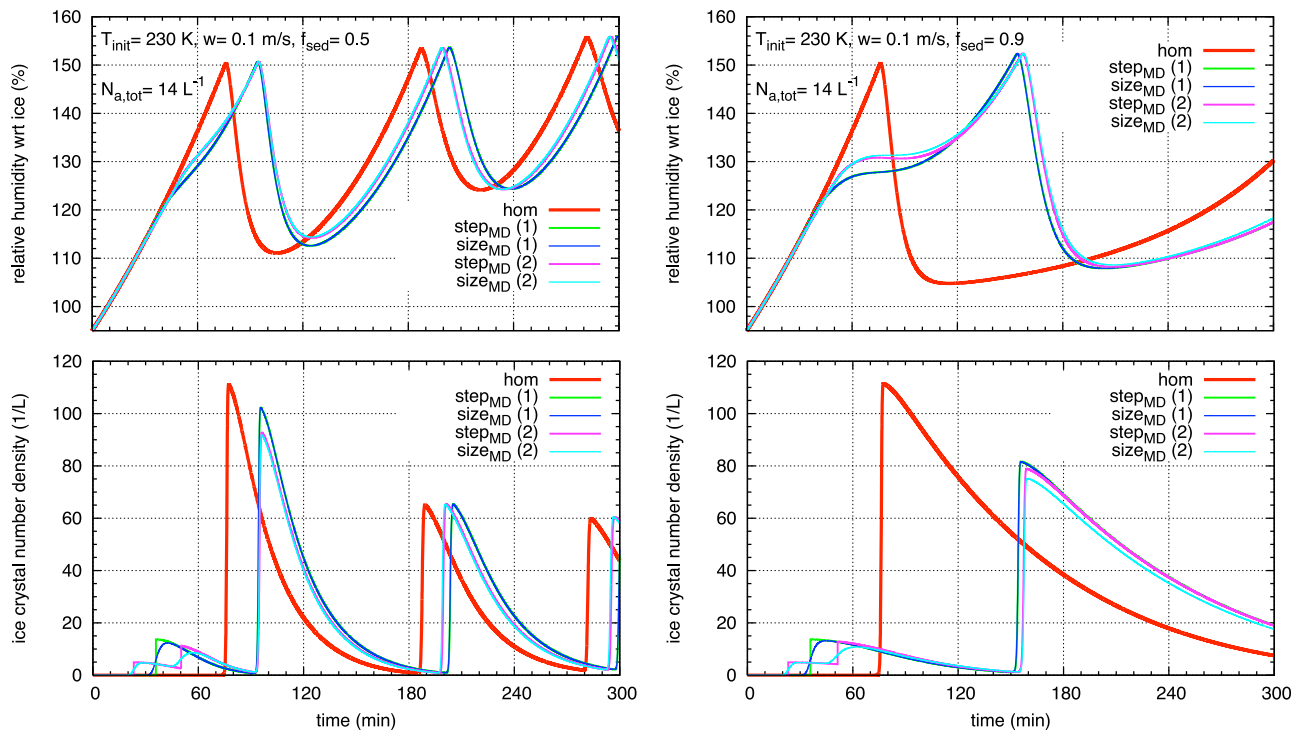


**Figure C2.** Two cases for determining the impact of heterogeneous nucleation on homogeneous nucleation for more “realistic” experiments of mineral dust (“hom, step<sub>MD</sub>(1), size<sub>MD</sub>(1), step<sub>MD</sub>(2), size<sub>MD</sub>(2)”) under normal IN background conditions ( $N_{a,tot} = 14$   $L^{-1}$ ). The evolution of (top) relative humidity over ice (in %) and (bottom) ice crystal number density (in  $L^{-1}$ ) is shown for different values of the sedimentation flux ratio: (left)  $f_{sed} = 0.5$  and (right)  $f_{sed} = 0.9$ . For all experiments an initial temperature of  $T_{init} = 230$  K and a constant updraft of  $w = 0.1$   $m s^{-1}$  is prescribed.

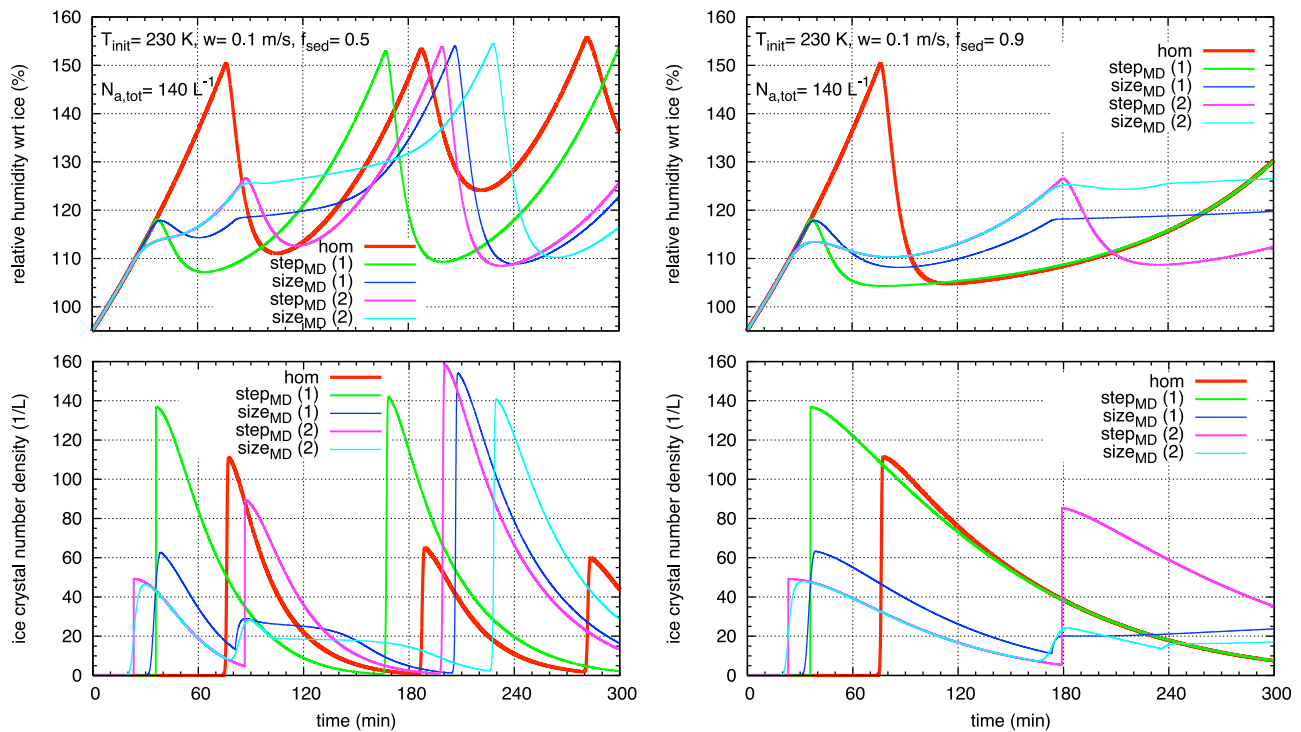


**Figure C3.** Same as Figure C2 but for polluted background conditions ( $N_{a,tot} = 140$   $L^{-1}$ ).

ground IN cases with only few IN types with very close freezing thresholds, the differences between the simulations remain small, although there is a strong impact on following homogeneous freezing events, compared to a pure homogeneous freezing simulation.

[105] For a polluted IN background things change drastically. Here, we can observe strong differences between the parameterizations. Qualitatively, we can identify the same features as for the idealized setups in a polluted background as stated in section 4.4. In case of sedimentation representative for the cloud top, mostly shifts in the homogeneous nucleation events occur. The shifted events might then be stronger than the comparable pure homogeneous nucleation event, as already explained in section 4.4. For sedimentation as representative for the middle of a cloud, homogeneous freezing is generally suppressed; the different IN parameterizations then determine the amount of formed ice crystals.

[106] Finally, we can state that our findings for the idealized simulation setups can be found again for the ‘realistic’ simulations. However, it should be noted here, that in the ‘realistic’ setup we only used two classes of mineral dust. Although the parameterizations might be more realistic, the overall setup is not. Usually, we have many different classes of IN with nucleation thresholds over the whole range from slightly supersaturated up to close homogeneous freezing thresholds. For an overview for more anthropogeneous substances we refer to Kärcher *et al.* [2007]. Thus, the idealized setup is probably a more ‘realistic’ simulation setup if typical conditions in the upper troposphere are investigated.

[107] **Acknowledgments.** We thank Klaus Gierens, Martina Krämer, Ulrike Lohmann, Thomas Peter, and Olaf Stetzer for fruitful discussions. This work was partly supported by the European Commission within the framework of the Marie Curie Fellowship “Impact of mesoscale dynamics and aerosols on the life cycle of cirrus clouds” (IMDALCC). This study contributes to the collaborative research center (SFB) “TROPEIS” of the German Research Foundation (DFG).

## References

- Archuleta, C. M., P. J. DeMott, and S. M. Kreidenweis (2005), Ice nucleation by surrogates for atmospheric mineral dust and mineral dust/sulfate particles at cirrus temperatures, *Atmos. Chem. Phys.*, *5*, 2617–2634.
- Barahona, D., and A. Nenes (2008), Parameterization of cirrus cloud formation in large-scale models: Homogeneous nucleation, *J. Geophys. Res.*, *113*, D11211, doi:10.1029/2007JD009355.
- Barahona, D., and A. Nenes (2009), Parameterizing the competition between homogeneous and heterogeneous freezing in cirrus cloud formation—Monodisperse ice nuclei, *Atmos. Chem. Phys.*, *9*, 369–381.
- Cantrell, W., and A. Heymsfield (2005), Production of ice in tropospheric clouds—A review, *Bull. Am. Meteorol. Soc.*, *86*, 795–807.
- Chen, J.-P., A. Hazra, and Z. Levin (2008), Parameterizing ice nucleation rates using contact angle and activation energy derived from laboratory data, *Atmos. Chem. Phys.*, *8*, 7431–7449.
- Chen, T., W. B. Rossow, and Y. Zhang (2000), Radiative effects of cloud-type variations, *J. Clim.*, *13*, 264–286.
- Comstock, J., R.-F. Lin, D. O. Starr, and P. Yang (2008), Understanding ice supersaturation, particle growth, and number concentration in cirrus clouds, *J. Geophys. Res.*, *113*, D23211, doi:10.1029/2008JD010332.
- Cziczo, D. J., P. J. DeMott, C. Brock, P. K. Hudson, B. Jessea, S. M. Kreidenweis, A. J. Prenni, J. Schreiner, D. S. Thomson, and D. M. Murphy (2003), A method for single particle mass spectrometry of ice nuclei, *Aerosol Sci. Technol.*, *37*, 460–470.
- Cziczo, D. J., D. M. Murphy, P. K. Hudson, and D. S. Thomson (2004a), Single particle measurements of the chemical composition of cirrus ice residue during CRYSTAL-FACE, *J. Geophys. Res.*, *109*, D04201, doi:10.1029/2003JD004032.
- Cziczo, D. J., P. J. DeMott, S. D. Brooks, A. J. Prenni, D. S. Thomson, D. Baumgardner, J. C. Wilson, S. M. Kreidenweis, and D. M. Murphy (2004b), Observations of organic species and atmospheric ice formation, *Geophys. Res. Lett.*, *31*, L12116, doi:10.1029/2004GL019822.
- Cziczo, D. J., D. S. Thomson, T. L. Thompson, P. J. DeMott, and D. M. Murphy (2006), Particle analysis by laser mass spectrometry (PALMS) studies of ice nuclei and other low number density particles, *Int. J. Mass Spectrom.*, *258*, 21–29.
- DeMott, P. J., D. C. Rogers, and S. M. Kreidenweis (1997), The susceptibility of ice formation in upper tropospheric clouds to insoluble aerosol components, *J. Geophys. Res.*, *102*, 19,575–19,584.
- DeMott, P., D. Cziczo, A. Prenni, D. Murphy, S. M. Kreidenweis, D. Thomson, R. Borys, and D. Rogers (2003a), Measurements of the concentration and composition of nuclei for cirrus formation, *Proc. Natl. Acad. Sci. U. S. A.*, *100*, 14,655–14,660.
- DeMott, P., K. Sassen, M. R. Poellot, D. Baumgardner, D. C. Rogers, S. D. Brooks, A. J. Prenni, and S. M. Kreidenweis (2003b), African dust aerosols as atmospheric ice nuclei, *Geophys. Res. Lett.*, *30*(14), 1732, doi:10.1029/2003GL017410.
- Eastwood, M. L., S. Cremel, C. Gehrke, E. Girard, and A. Bertram (2008), Ice nucleation on mineral dust particles: Onset conditions, nucleation rates and contact angles, *J. Geophys. Res.*, *113*, D22203, doi:10.1029/2008JD010639.
- Eidhammer, T., P. J. DeMott, and S. M. Kreidenweis (2009), A comparison of heterogeneous ice nucleation parameterizations using a parcel model framework, *J. Geophys. Res.*, *114*, D06202, doi:10.1029/2008JD011095.
- Fusina, F., P. Spichtinger, and U. Lohmann (2007), The impact of ice supersaturated regions and thin cirrus on radiation in the midlatitudes, *J. Geophys. Res.*, *112*, D24S14, doi:10.1029/2007JD008449.
- Gayet, J.-F., J. Ovarlez, V. Shcherbakov, J. Ström, U. Schumann, A. Minikin, F. Auriol, and A. Petzold (2004), Cirrus cloud microphysical and optical properties at southern and northern midlatitudes during the INCA experiment, *J. Geophys. Res.*, *109*, D20206, doi:10.1029/2004JD004803.
- Gierens, K. M. (2003), On the transition between heterogeneous and homogeneous freezing, *Atmos. Chem. Phys.*, *3*, 437–446.
- Haag, W., and B. Kärcher (2004), The impact of aerosols and gravity waves on cirrus clouds at midlatitudes, *J. Geophys. Res.*, *109*, D12202, doi:10.1029/2004JD004579.
- Hendricks, J., B. Kärcher, U. Lohmann, and M. Ponater (2005), Do aircraft black carbon emissions affect cirrus clouds on the global scale?, *Geophys. Res. Lett.*, *32*, L12814, doi:10.1029/2005GL022740.
- Hoyle, C., B. Luo, and T. Peter (2005), The origin of high ice crystal number densities in cirrus clouds, *J. Atmos. Sci.*, *62*, 2568–2579.
- Joos, H., P. Spichtinger, and U. Lohmann (2009), Orographic cirrus in a changing climate, *Atmos. Chem. Phys. Discuss.*, *9*, 8943–8991.
- Kajikawa, M., and A. Heymsfield (1989), Aggregation of ice crystals, *J. Atmos. Sci.*, *46*, 3108–3121.
- Kanji, Z. A., and J. P. D. Abbatt (2006), Laboratory studies of ice formation via deposition mode nucleation onto mineral dust and n-hexane soot samples, *J. Geophys. Res.*, *111*, D16204, doi:10.1029/2005JD006766.
- Kärcher, B. (2002), Properties of subvisible cirrus clouds formed by homogeneous freezing, *Atmos. Chem. Phys.*, *2*, 161–170.
- Kärcher, B. (2005), Supersaturation, dehydration, and denitrification in Arctic cirrus, *Atmos. Chem. Phys.*, *5*, 1757–1772.
- Kärcher, B., and U. Lohmann (2002), A parameterization of cirrus cloud formation: Homogeneous freezing of supercooled aerosols, *J. Geophys. Res.*, *107*(D2), 4010, doi:10.1029/2001JD000470.
- Kärcher, B., and U. Lohmann (2003), A parameterization of cirrus cloud formation: Heterogeneous freezing, *J. Geophys. Res.*, *108*(D14), 4402, doi:10.1029/2002JD003220.
- Kärcher, B., J. Hendricks, and U. Lohmann (2006), Physically-based parameterization of cirrus cloud formation for use in global atmospheric models, *J. Geophys. Res.*, *111*, D01205, doi:10.1029/2005JD006219.
- Kärcher, B., O. Möhler, P. DeMott, S. Pechtl, and F. Yu (2007), Insights into the role of soot aerosols in cirrus cloud formation, *Atmos. Chem. Phys.*, *7*, 4203–4227.
- Kay, J. E., M. Baker, and D. Hegg (2006), Microphysical and dynamical controls on cirrus cloud optical depth distributions, *J. Geophys. Res.*, *111*, D24205, doi:10.1029/2005JD006916.
- Kay, J. E., M. Baker, and D. Hegg (2007), Physical controls on orographic cirrus inhomogeneity, *Atmos. Chem. Phys.*, *7*, 3771–3781.
- Koenig, L. R. (1971), Numerical modeling of ice deposition, *J. Atmos. Sci.*, *28*, 226–237.
- Koop, T., B. Luo, A. Tsias, and T. Peter (2000), Water activity as the determinant for homogeneous ice nucleation in aqueous solutions, *Nature*, *406*, 611–614.

- Lin, R.-F., D. Starr, J. Reichardt, and P. DeMott (2005), Nucleation in synoptically forced cirrostratus, *J. Geophys. Res.*, *110*, D08208, doi:10.1029/2004JD005362.
- Liu, X., J. E. Penner, S. J. Ghan, and M. Wang (2007), Inclusion of ice microphysics in the NCAR Community Atmospheric Model Version 3 (CAM3), *J. Clim.*, *20*, 4526–4547.
- Lohmann, U., B. Kärcher, and J. Hendricks (2004), Sensitivity studies of cirrus clouds formed by heterogeneous freezing in the ECHAM GCM, *J. Geophys. Res.*, *109*, D16204, doi:10.1029/2003JD004443.
- Lohmann, U., P. Spichtinger, S. Jess, T. Peter, and H. Smit (2008), Cirrus cloud formation and ice supersaturated regions in a global climate model, *Environ. Res. Lett.*, *3*, 045022, doi:10.1088/1748-9326/3/4/045022.
- Marcolli, C., T. Peter, S. Gedamke, and B. Zobrist (2007), Efficiency of immersion mode ice nucleation on surrogates of mineral dust, *Atmos. Chem. Phys.*, *7*, 5081–5091.
- Meyers, M., P. DeMott, and W. Cotton (1992), New primary ice-nucleation parametrizations in an explicit cloud model, *J. Appl. Meteorol.*, *31*, 708–721.
- Minikin, A., A. Petzold, J. Ström, R. Krejci, M. Seifert, P. van Velthoven, H. Schlager, and U. Schumann (2003), Aircraft observations of the upper tropospheric fine particle aerosol in the Northern and Southern Hemispheres at midlatitudes, *Geophys. Res. Lett.*, *30*(10), 1503, doi:10.1029/2002GL016458.
- Möhler, O., et al. (2006), Efficiency of the deposition mode ice nucleation on mineral dust particles, *Atmos. Chem. Phys.*, *6*, 3007–3021.
- Peter, T., C. Marcolli, P. Spichtinger, T. Corti, M. B. Baker, and T. Koop (2006), When dry air is too humid, *Science*, *314*(5804), 1399–1402.
- Phillips, V. T. J., P. J. DeMott, and C. Andronache (2008), An empirical parameterization of heterogeneous ice nucleation for multiple chemical species of aerosol, *J. Atmos. Sci.*, *65*, 2757–2783.
- Pruppacher, H., and J. Klett (1997), *Microphysics of Clouds and Precipitation*, Kluwer Acad., Dordrecht, Netherlands.
- Ren, C., and A. R. Mackenzie (2005), Cirrus parametrization and the role of ice nuclei, *Q. J. R. Meteorol. Soc.*, *131*, 1585–1605.
- Richardson, M. S., et al. (2007), Measurements of heterogeneous ice nuclei in the western United States in springtime and their relation to aerosol characteristics, *J. Geophys. Res.*, *112*, D02209, doi:10.1029/2006JD007500.
- Rogers, D. C., P. J. DeMott, S. M. Kreidenweis, and Y. Chen (2001), A continuous flow diffusion chamber for airborne measurements of ice nuclei, *J. Atmos. Oceanic Technol.*, *18*, 725–741.
- Rotstayn, L. (1997), A physically based scheme for the treatment of stratiform clouds and precipitation in large-scale models.1. Description and evaluation of the microphysical processes, *Q. J. R. Meteorol. Soc.*, *123*, 1227–1282.
- Spichtinger, P., and K. Gierens (2009a), Modelling of cirrus clouds. Part 1a: Model description and validation, *Atmos. Chem. Phys.*, *9*, 685–706.
- Spichtinger, P., and K. Gierens (2009b), Modelling of cirrus clouds. Part 1b: Structuring cirrus clouds by dynamics, *Atmos. Chem. Phys.*, *9*, 707–719.
- Spichtinger, P., and K. Gierens (2009c), Modelling of cirrus clouds. Part 2: Competition of different nucleation mechanisms, *Atmos. Chem. Phys.*, *9*, 2319–2334.
- Spichtinger, P., K. Gierens, and H. Wernli (2005a), A case study on the formation and evolution of ice supersaturation in the vicinity of a warm conveyor belt's outflow region, *Atmos. Chem. Phys.*, *5*, 973–987.
- Spichtinger, P., K. Gierens, and A. Dörnbrack (2005b), Formation of ice supersaturation by mesoscale gravity waves, *Atmos. Chem. Phys.*, *5*, 1243–1255.
- Spichtinger, P., K. Gierens, and U. Lohmann (2006), Importance of a proper treatment of ice crystal sedimentation for cirrus clouds in large-scale models, paper presented at 12th Conference on Cloud Physics, Am. Meteorol. Soc., Madison, Wis.
- Stephens, G. (1983), The influence of radiative transfer on the mass and heat budgets of ice crystals falling in the atmosphere, *J. Atmos. Sci.*, *40*, 1729–1739.
- Stetzer, O., B. Baschek, F. Lüönd, and U. Lohmann (2008), The Zurich Ice Nucleation Chamber (ZINC)—A new instrument to investigate atmospheric ice formation, *Aerosol Sci. Technol.*, *42*, 64–74, doi:10.1080/02786820701787944.
- Stier, P., J. Feichter, E. Roeckner, S. Kloster, and M. Esch (2006), The evolution of the global aerosol system in a transient climate simulation from 1860 to 2100, *Atmos. Chem. Phys.*, *6*, 3059–3076.
- Wacker, U., and A. Seifert (2001), Evolution of rain water profiles resulting from pure sedimentation: Spectral vs. parameterized description, *Atmos. Res.*, *58*, 19–39.
- Welti, A., F. Luond, O. Stetzer, and U. Lohmann (2009), Influence of particle size on the ice nucleating ability of mineral dusts, *Atmos. Chem. Phys.*, *9*, 6705–6715.
- Zimmermann, F., S. Weinbruch, L. Schütz, H. Hofmann, M. Ebert, K. Kandler, and A. Wörzinger (2008), Ice nucleation properties of the most abundant mineral dust phases, *J. Geophys. Res.*, *113*, D23204, doi:10.1029/2008JD010655.

D. J. Cziczo, Atmospheric Sciences and Global Change Division, Pacific Northwest National Laboratory, Richland, WA 99352, USA. (daniel.cziczo@pnl.gov)

P. Spichtinger, Institute for Atmospheric and Climate Science, ETH Zurich, CHN 016.2, CH-8092 Zurich, Switzerland. (peter.spichtinger@env.ethz.ch)